JCI The Journal of Clinical Investigation

Expression of mitochondrial membrane-linked SAB determines severity of sex-dependent acute liver injury

Sanda Win, … , Tin A. Than, Neil Kaplowitz

J Clin Invest. 2019. https://doi.org/10.1172/JCI128289.

Research In-Press Preview **Hepatology**

SAB is an outer membrane docking protein for JNK mediated impaired mitochondrial function. Deletion of*Sab* in hepatocytes inhibits sustained JNK activation and cell death. Current work demonstrated that increasing SAB enhanced the severity of APAP liver injury. Female mice were resistant to liver injury and exhibited markedly decreased hepatic SAB protein expression versus males. The mechanism of SAB repression involved a pathway from ERα to p53 expression which induced *miR34a-5p*. *miR34a-5p* targeted the *Sab* mRNA coding region, repressing SAB expression. Fulvestrant or *p53* knockdown decreased *miR34a-5p* and increased SAB in females leading to increased injury from APAP and TNF/galactosamine. In contrast, ERα agonist increased p53 and *miR34a-5p* which decreased SAB expression and hepatotoxicity in males. Hepatocyte-specific deletion of *miR34a* also increased severity of liver injury in females, which was prevented by GalNAc-ASO knockdown of *Sab*. Similar to mice, premenopausal human females also expressed high hepatic p53 and low SAB levels while age-matched males expressed low p53 and high SAB levels, but there was no sex difference of SAB expression in postmenopause. In conclusion, the level of SAB expression determined the severity of JNK dependent liver injury. Females expressed low hepatic SAB protein levels due to an ERα-p53-*miR34a* pathway which repressed SAB expression, accounting for resistance to liver injury.

Expression of mitochondrial membrane-linked SAB determines severity of sex-dependent acute liver injury

Sanda Win[1*], Robert W.M. Min[1*], Christopher Q. Chen[1], Jun Zhang[2], Yibu Chen[3], Meng Li[3], Ayako Suzuki[4], Manal F. Abdelmalek[4], Ying Wang[4], Mariam Aghajan[5], Filbert W.M. Aung[1], Anna Mae Diehl[4], Roger J. Davis[6], Tin A. Than[1], Neil Kaplowitz[1]

[1]USC Research Center for Liver Disease, Keck School of Medicine, University of Southern California, Los Angeles, California, United States

[2]Department of Gastroenterology, Renmin Hospital of Wuhan University, Wuhan, China

[3]USC Libraries Bioinformatics Service, Norris Medical Library, University of Southern California, Los Angeles, California, United States

[4]Division of Gastroenterology, Department of Medicine, Duke University, Durham, North Carolina, United States

[5]Ionis Pharmaceuticals, Carlsbad, California, United States

[6] Howard Hughes Medical Institute and Program in Molecular Medicine, University of Massachusetts Medical School, Worcester, United States

* co-first authors

Disclosures: The authors have no relevant conflicts of interest to disclose.

Keywords: Apoptosis, necrosis, estrogen receptor-α, p53, miRNA-34a, acetaminophen toxicity, TNF/galactosamine, c-Jun-N-terminal kinase, SH3BP5

Correspondence:
Neil Kaplowitz, MD
Division of Gastroenterology and Liver Diseases
Department of Medicine, Keck School of Medicine
2011 Zonal Avenue, HMR 101
Los Angeles, CA 90033
E-mail: kaplowit@usc.edu
Ph: 1-323-442-5576

ABSTRACT

SAB is an outer membrane docking protein for JNK mediated impaired mitochondrial function. Deletion of *Sab* in hepatocytes inhibits sustained JNK activation and cell death. Current work demonstrated that increasing SAB enhanced the severity of APAP liver injury. Female mice were resistant to liver injury and exhibited markedly decreased hepatic SAB protein expression versus males. The mechanism of SAB repression involved a pathway from ERα to p53 expression which induced *miR34a-5p*. *miR34a-5p* targeted the *Sab* mRNA coding region, repressing SAB expression. Fulvestrant or *p53* knockdown decreased *miR34a-5p* and increased SAB in females leading to increased injury from APAP and TNF/galactosamine. In contrast, ERα agonist increased p53 and *miR34a-5p* which decreased SAB expression and hepatotoxicity in males. Hepatocyte-specific deletion of *miR34a* also increased severity of liver injury in females, which was prevented by GalNAc-ASO knockdown of *Sab*. Similar to mice, premenopausal human females also expressed high hepatic p53 and low SAB levels while age-matched males expressed low p53 and high SAB levels, but there was no sex difference of SAB expression in postmenopause. In conclusion, the level of SAB expression determined the severity of JNK dependent liver injury. Females expressed low hepatic SAB protein levels due to an ERα-p53-*miR34a* pathway which repressed SAB expression, accounting for resistance to liver injury.

INTRODUCTION

C-Jun-N-terminal kinase (JNK) signaling is important in liver injury scenarios (1-8) and appears to involve the interaction of activated JNK and an outer mitochondrial membrane target, SAB (also known as SH3BP5) (9). This interaction has been extensively studied in the acetaminophen (APAP) hepatotoxicity model (10, 11), as well as other models (12-14). A marked sex difference in susceptibility to toxicity has been well-documented in APAP treated mice (female resistance) but the mechanism for this sex difference is not fully understood (15-17). We hypothesized that this sex difference may not be unique to APAP and may suggest a sex difference in the contribution of the interaction of JNK with SAB.

The mechanism of APAP hepatotoxicity involves the conversion of a small proportion of APAP to a toxic intermediate, NAPQI, which initially depletes glutathione (GSH), leaving unprotected protein thiols which undergo covalent binding especially in mitochondria. This impairs mitochondrial function to a sufficient extent to release reactive oxygen species (ROS) which activate the MAPK cascade leading to JNK activation (18). JNK then binds to and phosphorylates SAB (SH3BP5) on the outer membrane. SAB then releases a protein phosphatase (PTPN6) bound to the intermembrane face of SAB leading to its interaction with P-SRC (active) facilitated by the inner membrane platform protein DOK4. P-SRC is then inactivated leading to inhibition of mitochondrial electron transport (which requires activated SRC) and increased ROS release, sustaining JNK activation and amplifying ROS exposure in mitochondria (11, 12), and ultimately leading to necrosis through mitochondrial permeability transition pore (MPT) (19, 20). Pivotal in this context is the maintenance of sustained JNK activation. This pathway, referred to as the JNK-SAB-ROS activation loop, is also important in

the mechanism of tumor necrosis factor (TNF)-induced apoptosis of hepatocytes sensitized by treatment with D-galactosamine (GalN) in vivo or actinomycin D (ActD) in vitro (10, 11). In this circumstance, sustained JNK activation modulates the BCL family of gatekeepers of outer mitochondrial membrane permeability by activating BID, BAX, BIM, PUMA and inactivating BCL-X_L and MCL-1 (21-26). We previously showed that hepatocyte specific SAB deletion in male mice prevented sustained JNK activation and liver injury in the APAP and GalN/TNF induced liver injury models. Since no sex difference in total hepatic JNK1 and JNK2 but decreased sustained JNK activation in females was previously reported in the APAP injury model (17), we hypothesized that sex dependent regulation of SAB expression may account for the sex difference in susceptibility to acute liver injury. More importantly, if this were to be the case it would provide a unique opportunity to examine the regulation of SAB expression for the first time and to determine the importance of the level of SAB expression in the susceptibility to and severity of acute liver injury.

RESULTS

Resistance of female mice to acute liver injury is associated with low SAB expression

Since the liver injury from APAP is known to be more severe in the N than J substrain of C56BL/6 mice (27, 28), our first objective was to confirm that the previously reported resistance to APAP toxicity in the female C57BL/6J strain also extends to the C57BL/6N strain. The N substrain females exhibited markedly decreased histologic necrosis and ALT levels compared to littermate males (Figure 1A) accompanied by decreased sustained P-JNK activation and mitochondrial translocation but no sex difference in total JNK expression (Figure 1C). Furthermore, we confirmed prior reports that there is no sex difference in basal hepatic GSH levels or GCLC expression (Figure S1, A and B). Furthermore the reported and confirmed greater recovery of GSH in females at 4 hour (Figure S1A) corresponds with decreased P-JNK and injury (Figure 1). GCLC protein level did not increase or decrease in females but rapidly declined in males before significant necrosis (Figure S1C), as we reported previously in males (29). Furthermore, there was no sex difference in the rate of GSH recovery following depletion by nontoxic phorone (Figure S1F) suggesting no intrinsic sex difference in GSH synthesis. In addition, as reported in B6J substrain, there was no sex difference in APAP metabolism to NAPQI as reflected in APAP protein adduct formation in the B6N substrain (Figure S1G). Nevertheless, because of the possibility that there may be inherent sex differences in other aspects of drug metabolism and antioxidant defense, we examined the GalN/TNF model of innate immune mediated apoptotic cell death which is independent of drug metabolism and GSH. Again, we observed marked protection in female mice with respect to liver injury and JNK activation (Figure 1, B and D). In addition APAP induced greater dose related (0, 100, 200, 300

mg/kg) liver injury in males versus females as reflected in serum ALT elevation (Figure S1D) and there was a direct correlation between ALT and P-JNK at 4hours after APAP (300mg/kg) (Figure S1F). Cell autonomous killing of primary mouse hepatocytes (PMH) by APAP and ActD/TNF was significantly greater in males versus females (Figure S1, H and I). In addition using PMH, we examined two other models in which toxicity is JNK and SAB dependent, i.e. tunicamycin (severe ER stress) (Figure S1K) and palmitic acid (Figure S1J) induced apoptosis, and we observed a significant decrease in cell death in female versus male PMH. In addition, there was no sex difference in basal expression of GRP78, PERK, ATF6, IRE1α, ATF2, c-JUN, MCL-1 or BCL-X_L (Figure S2).

The results in both APAP and GalN/TNF models of acute injury showed marked suppression of both P-JNK translocation to mitochondria and sustained P-JNK activation in the cytoplasm in female mice. The cause of sustained of P-JNK is release of ROS from mitochondria due to the intramitochondrial signaling pathway which leads to the dephosphorylation of P-SRC in the mitochondrial intermembrane space (11). Therefore, we examined sex difference in mitochondria SRC inactivation, which was also blunted in both injury models in females (Figure 1 C,D). This suggested that mitochondria of females are resistant to the effect of P-JNK. To support this, we measured the direct inhibitory effect of P-JNK on normal mitochondrial respiration. As we reported previously, P-JNK interaction with normal mitochondria inhibits OCR in liver mitochondria from males. In comparison, female liver mitochondria were resistant to the effect of P-JNK (Figure 2A and S3A). In addition, isolated mitochondria from male livers loaded with MitoSox (detection of $O_2^{\bullet-}$) generated a significantly greater ROS response to P-JNK than females (Figure 2B). There was no difference in mitochondrial GSH depletion in male

versus female at 1 or 2 hours after APAP (Figure S3B) and OCR was markedly impaired in mitochondria of males at these time points but was unaffected in females (Figure S3C). Since we have previously shown that the OCR and ROS responses to P-JNK are SAB-dependent (11, 12), we hypothesized that there is a sex difference in SAB expression. Indeed, liver mitochondria of females expressed SAB at <20% of the levels in male littermates (Figure 2C) but interestingly exhibited similar levels of hepatic *Sab* mRNA (Figure S3D). In addition, SAB protein remained constant during estrus cycle (Figure S3E). Since we previously showed that *Sab*$^{i\Delta Hep}$ male mice are resistant to the toxic effect of APAP and GalN/TNF, we hypothesized that the likely explanation for the resistance of females in these two models is due predominantly to the lower expression of SAB in females. The absence of a sex difference in *SAB* mRNA suggested post-transcriptional regulation of *SAB* (see below).

Importantly, a similar sex difference in SAB expression was observed in human liver samples. Samples of male and females were matched for age and BMI and pre- versus post-menopausal females were confirmed by estrogen and FSH levels. Biopsies were done for clinical indications so that mild ALT elevations and nonspecific histologic abnormalities were present. Samples for comparison of males and females were paired for age and sex according to menopausal status. A representative immunoblot of SAB expression of matched male and pre-menopausal females (Figure 2D) and a plot of normalized expression of SAB (Figure 2E) demonstrate markedly lower SAB expression in premenopausal females but no sex difference in post-menopause and no change in young versus older men.

Overexpression of SAB increases susceptibility to APAP toxicity in males

To test whether the level of SAB expression is a major determinant of acute liver injury, we next determined the effect of increasing SAB expression using Ad-*SAB* which contains the *SAB* cDNA (coding region) driven by CMV promoter. In wild type male mice, increasing doses of Ad-*SAB* increased SAB expression in the liver (Figure 3A) and this was accompanied by enhanced histologic liver necrosis and ALT levels in response to a low dose of APAP (150mg/mg) (Figure 3B). In addition, increasing Ad-*SAB* expression was associated with increased P-JNK 4 hours after APAP (Figure S3F) and this correlated with ALT levels in individual mice (Figure S3G). However, when we repeated this in female littermates, no increase in SAB expression was observed (Figure 4A) and the mice remained resistant to APAP-induced liver injury (not shown).

To further assess the importance of the level of SAB expression in determining the extent of liver injury we expressed SAB with increasing doses of Ad-*SAB* in *Sab*$^{i\Delta Hep}$ male mice (Figure 3C). This restored the susceptibility to APAP necrosis (absent in *Sab*$^{i\Delta Hep}$ mice), and lead to increased APAP necrosis and serum ALT in relationship to increasing viral dose (Figure 3D). To test the possibility that SAB is mediating a JNK-independent mechanism of toxicity, we assessed the effect of SAB overexpression in *Jnk1/2*$^{i\Delta Hep}$ mice. Inducible double knockout of Jnk 1 and 2 with AAV8-TBG-Cre in C57B6J *Jnk1/2*$^{f/f}$ mice (Figure 3E) conferred marked protection against APAP (600mg/kg); since J substrain is resistant to APAP (27, 28) we used a high dose of APAP to insure not missing a protective effect of *Jnk* deletion (Figure 3F*). Jnk1* and *2* deletion (*Jnk1/2*$^{i\Delta Hep}$) had no effect on SAB levels (Figure 3E). Concomitant overexpression of SAB (versus control) did not reverse the resistance to APAP in *Jnk1/2*$^{i\Delta Hep}$ mice (Figure 3F). Therefore, these data indicate that there is no JNK-independent mechanism for the effect of increased SAB overexpression on APAP toxicity. Thus, two important conclusions derive from

the results in Figure 3: (a) the level of SAB expression directly correlates with the extent of liver injury in response to APAP, indicating that level of SAB expression is a key checkpoint in determining the severity of liver injury; (b) JNK is necessary for SAB to increase susceptibility to liver injury and vice versa.

ERα inhibition reverses the resistance to SAB expression and APAP toxicity in female mice

As noted above, we attempted to reverse the resistance of female littermates by overexpressing SAB, but increasing doses of the same Ad-*SAB* as used in males did not increase the SAB levels in female liver (Figure 4A) and did not increase susceptibility to APAP or GalN/TNF (not shown). Estrogen accounts for many downstream sex differences. Estrogen effects may be dependent or independent of estrogen receptors (ER) (30). ER is present in two isoforms: ERα and ERβ as well as a membrane form (GPER). ERα is the main form in liver (31, 32) and is expressed at higher levels in females than males. Both ERβ and GPER are not detectable in liver (32, 33). To test if ERα plays an important upstream role in low SAB expression, we treated female mice with fulvestrant, an ER antagonist which destabilizes ER (34, 35). When female mice were treated with fulvestrant, the levels of ERα decreased and SAB levels increased in a fulvestrant dose dependent fashion (+: 2mg/kg, ++: 5mg/kg) (Figure 4B). PMH after in vivo treatment with fulvestrant exhibited enhanced P-JNK activation in response to APAP (Figure S4A). To further clarify whether the lack of Ad-*SAB* mediated expression in females is ERα dependent, we assessed the ability of fulvestrant to unmask Ad-*SAB* expression in females. Indeed, fulvestrant treatment in female mice before and following Ad-*SAB* lead to increased expression of Ad-*SAB* in female liver (Figure 4C) and reversed the resistance of female

mice to APAP toxicity (Figure 4D); the females then exhibited markedly increased histologic necrosis and ALT levels.

ERα activation decreases SAB expression and susceptibility to acute liver injury in male mice

To further define the role of ERα in the mechanism for sex difference in SAB levels, we treated male mice in vivo with a well-characterized potent and specific ERα chemical ligand activator, propylpyrazole triol (PPT), which does not activate ERβ (36, 37). Indeed, PPT treatment for five days markedly decreased SAB protein expression (Figure 4E) but not *Sab* mRNA (Figure S4B). PPT markedly protected male mice from both APAP and TNF/GalN toxicity as reflected in histologic injury and ALT levels in vivo (Figure 4, F and G).

To further assess the cell autonomous effect of the ERα agonist, PPT, we isolated hepatocytes from males after in vivo treatment of PPT or vehicle. The PMH cultures were then exposed to APAP or ActD/TNF. In both models, PPT pretreatment in vivo with resulting SAB depletion (Figure 4H) protected from PMH cell death accompanied by inhibition of sustained JNK activation in response to APAP or ActD/TNF (Figure 4, I and J). Furthermore, PPT pretreatment of male mice in vivo protected against PMH cell death due to tunicamycin (Figure S4C) and palmitic acid (Figure S4D) and decreased palmitic acid induced sustained JNK activation (Figure S4E). In addition, treatment of normal male hepatocytes with ERβ agonist (DPN) or androgen receptor agonist (BMS) did not affect SAB expression (Figure S4F). Therefore, the findings in Figure 4 suggest that SAB repression is mediated by ERα and activation of ERα consequently leads to suppression of sustained JNK activation and acute liver and cellular injury in males, while inactivation of ERα increases SAB expression and P-JNK

activation in females and unmasks the ability of Ad-*SAB* to restore susceptibility to liver injury in females.

miR34a targets *Sab* mRNA

As noted above, when we attempted to overexpress Ad-*SAB* in female mice, no increase in SAB expression was observed and the mice remained resistant with no increase in APAP induced liver injury. The basal resistance of female mice to the expression of Ad-*SAB* strongly suggested interference with SAB expression at the post-transcriptional level. The results in male mice treated with ERα agonist and in female treated with ER degrader supported the importance of ERα in upstream regulation of SAB. Furthermore, despite the large difference in SAB protein expression, there was no difference in hepatic *Sab* mRNA levels in females versus males. Taken together the findings lead us to the hypothesis that ERα, either directly or indirectly via an intermediate may regulate the expression of a miRNA which is targeting the *SAB* mRNA coding region of the Ad-*SAB* cDNA. Therefore, we performed miRNAseq analysis of liver samples from untreated male and female littermates. The results are shown as a volcano plot comparing littermate females to males (Figure 5A). Three miRNAs stood out as highly significant as reflected in >3fold higher levels in females. However, only one targets *Sab* mRNA, i.e. miR34a-5p, which is predicted to target the coding region (Figure 5B); since Ad-*SAB* cDNA does not contain a 3′-untranslated sequence, we expected that a miRNA would have to target the coding region. The sex difference in miR34a-5p was confirmed by qPCR (Figure 5C). To confirm the capability of miR34a-5p to repress SAB levels, we expressed miR34a-5p in HEK293 cells and observed decreased SAB protein (Figure 5D).

ERα regulates p53 which increases miR34a-5p

Since miR34a-5p was a likely candidate to repress translation of *Sab* mRNA, we next addressed the link between ERα and miR34a-5p. Two important facts were derived from prior publications: miR34a expression is transcriptionally regulated by p53 in other contexts and ERα is known to regulate p53 expression (38). Therefore, we examined p53 levels in males versus females and found significantly higher levels of hepatic p53 in female liver, both in mice and premenopausal human females (Figure 5, E and F). Thus, there was a sex dependent inverse relationship between p53 and SAB (Figure 1, G and H; Figure 5,E and F). We therefore determined the effect of ERα agonist (PPT) treatment in male mice and ERα antagonist (fulvestrant) treatment on p53 expression in females. Hepatic p53 was increased after PPT treatment of male mice and dose dependently decreased after fulvestrant treatment of females (Figure 5G). These data confirmed the regulation of p53 expression by estrogen.

After confirming the link between ERα and p53, we assessed the effect of knockdown of p53 in vivo using p53 antisense oligonucleotide (ASO) versus scrambled ASO control. Knockdown of p53 increased SAB expression in both males and females. Interestingly, p53 and SAB levels in females after knockdown of p53 were comparable to the basal levels in male controls (Figure 6A). As expected, p53 knockdown lead to decreased miR34a-5p levels in both male and female littermates (Figure 6B), which was accompanied by increased SAB levels (Figure S5A). We also confirmed that p53-ASO (ASO#2) targeting a different locus of *p53* mRNA also enhanced APAP toxicity (Figure S5B). As seen with SAB, the level of miR34a-5p in females after p53 knockdown was nearly identical to the basal male control. Conversely, to see if increased p53 expression and activation would repress SAB, we treated HepG2 cells with

sublethal dose of doxorubicin (induction of p53 by DNA damage) and HDAC inhibitor, Trichostatin A (increased acetyl-p53) as previously described (39-41) and observed SAB expression was markedly decreased after treatment, confirming upregulation of p53 leads to downregulation of SAB (Figure S5C).

We examined SIRT1 expression as it is known to be repressed by miR34a-5p (42). Also SIRT1 can de-acetylate p53 and somewhat inhibit its activity (43, 44). However, unexpectedly, the basal expression of SIRT1 and acetyl-p53 were both greater in female mouse liver, despite the lower SAB expression (Figure 6A and S5D). Also female humans exhibited higher hepatic SIRT1 levels (Figure S5E). However, despite the differences in basal levels, p53 knockdown decreased *miR34a* and increased SAB and SIRT1 protein expression in both males and females (Figure 6, A and B).

To further confirm the key role of p53 in ERα mediated repression of SAB, treatment of PMH from male mice with PPT after in vivo treatment with *p53* ASO was examined. Scrambled ASO pretreatment did not alter the repression of SAB by the ERα agonist, PPT (Figure 6C). PPT treatment of male control hepatocytes increased p53 levels, directly demonstrating regulation of p53 expression by activation of ERα (Figure 6C). However, *p53* ASO pretreatment and efficient knockdown of p53 prevented PPT mediated repression of SAB expression (Figure 6C). Importantly, *p53* knockdown did not unmask an alternative mechanism of ERα mediated PPT repression of SAB as the increased SAB expression after *p53* knockdown was not inhibited by PPT activation of ERα (Figure 6C). Therefore, ERα regulates p53 expression which increases miR34a leading to repression of SAB.

We recently reported that there was an inverse relationship between acute liver injury from APAP in male mice with p53 inhibition or knockdown leading to increased P-JNK and toxicity while p53 activation lead to decrease P-JNK and protection (45). Therefore, we extended our studies by examining the effect of *p53* knockdown on liver injury in female mice treated with APAP or GalN/TNF. In both injury models *p53* knockdown lead to increased injury in both male and female *Sab*$^{f/f}$ controls which was most striking in females and lead to comparable toxicity as in males (Figure 6, D and E). Increased APAP toxicity in female *miR34*$^{i\Delta Hep}$ mice was accompanied by enhanced P-JNK in the early time course (Figure S6A). Of note, the enhanced JNK activation after APAP in female *miR34*$^{i\Delta Hep}$ mice was accompanied by impaired GSH recovery (Figure S6B) whereas *miR34a-5p* mimic treated males (decreased SAB and P-JNK) exhibited enhanced GSH recovery (Figure S6C). These findings support the conclusion that the difference in GSH recovery is not an intrinsic sex-dependent phenomenon but is secondary to the effect of SAB-JNK and severity of injury. In addition, the marked resistance of *Sab*$^{i\Delta Hep}$ male and female mice to APAP and GalN/TNF was not overcome by *p53* knockdown (Figure 6, D and E) indicating that the worsening of liver injury after p53 inhibition in both models and sex is dependent on the expression of SAB and not due to an alternative p53 regulated protective mechanism.

Expression of miR34a-5p directly determines the severity of acute liver injury

Having established a pathway from ERα to p53 to *miR34a-5p* to SAB repression, further evidence was required to conclusively link *miR34a-5p* to the protection from liver injury. Therefore, we treated male mice with Ad-*miR34a-5p* mimic which lead to increased *miR34a-5p* level (Figure S7A) and was accompanied by a marked decrease in SAB protein to low but

comparable levels as found in untreated females (Figure S7B). However, SAB mRNA levels were not changed by Ad-*miR34a-5p* mimic (Figure S7C). Under these conditions, the *miR34a-5p* mimic was successful in markedly protecting male mice against APAP and GalN/TNF induced liver injury (histologic injury and serum ALT) compared to the control (Figure S7D). In contrast, we compared female *miR34a*$^{f/f}$ mice treated with AAV8-TBG-GFP (control) or AAV8-TBG-Cre. The *miR34a*$^{i\Delta Hep}$ females exhibited extremely low *miR34a* levels (Figure 7A). Inducible knockout of *miR34a* lead to increased SAB protein levels (Figure 7B). Interestingly, *miR34a*$^{i\Delta Hep}$ mice exhibited increased p53 levels consistent with previous reports that *miR34a* represses p53 in HepG2 cell (46), but increased p53 exerted no protection against liver injury in the *miR34a*$^{i\Delta Hep}$ mice. As expected SIRT1 levels were decreased by the *miR34a-5p* mimic but no increase was seen in *miR34a*$^{i\Delta Hep}$ (Figure 7B and S7B). In both APAP and GalN/TNF injury models, *miR34a*$^{i\Delta Hep}$ exhibited markedly enhanced liver injury (histologic injury and serum ALT) (Figure 7C). In fact, the injury in female *miR34a*$^{f/f}$ mice treated with AAV8-TBG-Cre (Figure 7C) was comparable to APAP and GalN/TNF treated male controls (Ad-miR-GFP) (Figure S7D). *miR34a*$^{i\Delta Hep}$ female mice express increased SAB protein but not *Sab* mRNA (Figure S7E) again consistent with *miR34a* repressing the translation of *Sab* mRNA to protein. Finally to test whether the de-repression of *Sab* in *miR34a*$^{i\Delta Hep}$ is the mechanism for enhanced liver injury, we knocked down *Sab* in female *miR34a*$^{i\Delta Hep}$ mice using GalNAc-*Sab* ASO compared to GalNAc-scrambled control ASO (Figure 7D). The GalNAc derivative increases ASO potency and selectively targets hepatocytes through the asialoglycoprotein receptor (47). Treatment with the GalNAc-*Sab* ASO in vivo depleted SAB in hepatocytes but had no effect on SAB in nonparenchymal cells (Figure S7F). The female *miR34a*$^{i\Delta Hep}$ mice treated with scrambled ASO had no effect on SAB level or the enhanced injury

response to APAP or GalN/TNF, whereas the GalNAc-*Sab* ASO markedly decreased hepatocyte SAB expression and prevented enhanced liver injury in the *miR34a*$^{i\Delta Hep}$ female mice as seen with parent Sab ASO (Figure 7D; Figure S7, G and H).

DISCUSSION

The JNK-SAB-ROS activation loop plays a critical role in sustaining JNK activation (9). Prolonged JNK activation can promote cell death by phosphorylation of transcription factors which increase expression of BH3 members of BCL2 family (eg. PUMA) (25, 48), or by directly activating pro-apoptotic BCL2 family members (eg. BAX, BID) or inactivating anti-apoptotic proteins (eg. MCL-1, BCL-X_L) (21-24). SAB plays a pivotal role in mediating mitochondrial ROS production (11, 12), but very little is known about the regulation of SAB expression. We previously reported that *Sab* knockdown or hepatocyte-specific inducible deletion of *Sab* markedly protected against liver injury in models in which injury is JNK dependent (10, 11). Thus far, our understanding of the role of SAB is based upon its absence versus presence. However it is important to understand if SAB expression is regulated under certain physiological conditions and if this influences the susceptibility to and severity of liver injury. We approached this question by examining SAB expression in male versus female mice because it has been reported that females are resistant to APAP toxicity and exhibit lower sustained JNK activation and mitochondrial translocation but exhibit no differences in expression of total JNK compared to males. Therefore, we considered this a potentially informative scenario to address the role of SAB expression. In addition, we examined the restoration of SAB expression to different levels in *Sab*$^{i\Delta Hep}$ mice to examine the relationship of the level of SAB expression and the severity of liver injury. We confirmed the resistance of female mice to APAP injury. However, females were also resistant to the toxicity of GalN/TNF in vivo, another JNK dependent acute liver injury model, which is independent of drug metabolism and GSH status. In addition, cultured PMH from females were resistant to apoptotic cell death from tunicamycin

and palmitic acid. These findings strengthened the hypothesis that there might be a difference in basal mitochondrial SAB expression contributing to the resistance of female mice to liver injury compared to males. SAB is the binding target and substrate of P-JNK (49). Supporting the possibility that there may be a sex difference in SAB expression, liver mitochondria from females were less susceptible to P-JNK + ATP induced inhibition of respiration and enhancement of ROS production. Indeed, SAB protein levels in female mouse mitochondria were <20% of the male levels. Importantly, the liver of humans with near normal histology revealed a similar sex difference in SAB expression. The correlation between resistance to liver injury with low SAB levels lead us to address the mechanism and importance of decreased SAB expression in females and to gain new insight into the regulation and importance of SAB.

To elucidate the mechanism for SAB repression in females, we assessed the effect of activating ERα in males and inactivating ERα in females. ERα is the major target of estrogens and is expressed at high levels in females. ERα agonist treatment of males lowered SAB expression and ERα antagonist increased SAB expression in females. In males the activation of ERα was accompanied by resistance to acute liver injury due to APAP and GalN/TNF whereas the opposite was observed in females treated with ERα antagonist.

To address the importance of SAB expression level in determining the severity of liver injury in males as well as sex difference in susceptibility, we first overexpressed SAB in wild type male mice and *Sab*$^{i\Delta Hep}$ mice using adenoviral (Ad) *SAB* cDNA. A direct relationship between the level of SAB expression and liver injury from APAP was observed. Though most research in liver injury models supports a pivotal role of JNK in mediating hepatocellular death, one recent study found that mice with liver specific embryonic knockout of *Jnk1* crossed with global *Jnk2*

knockout mice exhibited increased APAP-induced liver injury suggesting JNK might be protective (50). Since this study and ours used different approaches to delete *Jnk1/2*, embryonic versus inducible, they are not directly comparable. Recently, Zoubek et al (51) found a hepatocyte specific protective role of JNK2 in ibuprofen-induced acute liver failure model (worsened with JNK2 knockdown). Therefore, study of the relative contribution of JNK1 versus JNK2 in the models we have employed will be of great interest and are planned for the future. However, the work of Cubero et al does raise an important question relevant to our work on SAB as to whether the unequivocal participation of SAB in liver injury might be due to an alternative JNK-independent mechanism for SAB dependence in acute liver injury. To address this we crossed *Jnk1*$^{f/f}$ and *Jnk2*$^{f/f}$ mice (C57B6J strain) and injected AAV8-TBG-CRE in two month old double floxed adult mice to induce combined hepatocyte *Jnk1* and *2* deletion in the livers of adult males. Deletion of both *Jnk1* and *2* in these mice caused striking resistance to APAP but had no effect on SAB expression. We then overexpressed SAB in the *Jnk1/2*$^{i\Delta Hep}$ mice but found no restoration of susceptibility to APAP toxicity. These findings confirm that enhanced APAP toxicity after increased SAB expression is JNK dependent. Furthermore, the findings indicated that it is unlikely that a JNK-independent mechanism accounts for the role of SAB in liver injury.

Studies by the Chambers lab are also consistent with the importance of the level of SAB expression in cell injury. Overexpression of SAB in H9c2 cardiac cells, and Hela cells sensitized to toxicity from drugs such as imatinib and chemotherapy drugs (52, 53). Furthermore, they demonstrated that in a panel of ovarian cancer cells, the level of SAB expression correlated with the chemo-toxicity: SAB level correlated with high susceptibility and overexpression of SAB in a

chemo-resistant cell line increased sensitivity to chemotherapy drug (54). These studies and the present work indicate that the level of mitochondria SAB dictates the magnitude of JNK activation and signaling under toxic stress. Of note, Pauel et al found that ovarian cancer cells with high SAB expression were primed for apoptosis as reflected in decreased pro-survival BCL-2 proteins and increased BH3-only proteins on mitochondria. These findings in cultured cancer cells differ from our results in the liver showing no changes in BCL-2 proteins probably because under basal conditions SAB overexpression does not activate JNK or c-JUN in vivo in the liver.

Having established the relationship between SAB expression and severity of liver injury in males, we then attempted to overexpress SAB in females, expecting to demonstrate that overexpression of SAB in females would eliminate the sex difference. However, we observed no increase in either SAB levels or susceptibility to liver injury after administering Ad-*SAB*. Since the *SAB* cDNA is derived from *SAB* mRNA corresponding to coding region of the *SAB* gene, a post-transcriptional mechanism for repression of *SAB* was suspected. Indeed, a miRNA sequence comparison of male and female littermates under basal conditions revealed several miRNA that were much more highly expressed in female livers. Among these, only miR34a-5p was predicted to target *Sab* mRNA (at the coding region corresponding to exon 4). When ERα was inhibited by fulvestrant in female mice, the Ad-*SAB* mediated expression of SAB was unmasked and females became sensitized to APAP and GalN/TNF liver injury. Since the sex difference in SAB protein expression was not accompanied by a difference in *Sab* mRNA levels, a repression of translation of *Sab* mRNA was strongly suggested.

miR34a-5p is known to be transcriptionally regulated by p53 (46, 55, 56). Interestingly, we found that p53 levels were significantly higher in liver tissue of female mice and humans

compared to males. Furthermore, the ERα agonist increased p53 expression in males and the ERα antagonist decreased p53 in females, confirming that ERα regulates p53 which then increases *miR34a-5p* expression. We recently reported that p53 had a protective effect against APAP in male mice (45). We now show that p53 induces the expression of *miR34a-5p* which represses SAB and protects against JNK activation and liver injury. Although JNK is known to phosphor- activate p53 (57-59), the repression of SAB inhibits sustained JNK activation and therefore would minimize an effect on p53- induced cell death.

The importance of *miR34a-5p* was directly confirmed by expressing a mimic in males, which lead to resistance to liver injury, and by deletion of *miR34a* gene in the liver of females, which lead to greatly increased susceptibility to liver injury. These effects correlated with the levels of sustained JNK activation. The *miR34a*$^{i\Delta Hep}$ mice exhibit de-repression of SAB and enhanced acute liver injury which was abrogated by *Sab* knockdown indicating that major factor in the influence of *miR34a* on acute APAP and GalN/TNF liver injury is its effect on SAB protein expression and SAB is indispensable for APAP and GalN/TNF hepatotoxicity. Though the *miR34a-5p* mimic decreased SAB protein and the knockout of *miR34a* increased SAB protein, neither changed *Sab* mRNA levels which further supports the hypothesis that *miR34a* inhibits translation of *Sab* mRNA rather than causing degradation. Importantly, treatment of *miR34a*$^{i\Delta Hep}$ mice with GalNAc-*Sab*-ASO causing hepatocyte specific efficient knockdown of *Sab* prevented the enhanced liver injury, conclusively indicating that *miR34a* exerts its effect on hepatotoxicity through regulation of SAB.

In parallel to mice, human liver samples exhibited a similar reciprocal relationship between p53 and SAB with premenopausal females exhibiting high p53 and low SAB and males

exhibiting low p53 and high SAB. Although this suggests that our findings may be relevant to humans, we could find no conclusive evidence that the decreased susceptibility of female mice to acute liver injury does or does not translate to humans because of a paucity of data comparing susceptibility of males and females. A study using male and female hepatocytes exposed to different hepatotoxic drugs showed sex differences in certain parameters in high content imaging in a drug specific fashion (60). In the case of APAP, toxicity was greater in pooled hepatocytes in suspension from postmenopausal females and was comparable to males, consistent with our findings. However, for other drugs female hepatocytes were more susceptible. However, the effects of sex on the metabolism of these drugs was not examined and overall the exposures were performed at very short times (up to 6 hours) making the results difficult to compare to in vivo. In addition, greater female representation in APAP-induced acute liver failure (ALF) database has been reported but this may be explained by sex difference in the incidence of overdose (61, 62). However, evidence of sex difference in human liver injury (female resistance) in ischemia/reperfusion injury and α1–antitrypsin deficiency has been described (63-65). Thus, though the reciprocal relationship between p53 and SAB expression found in mouse liver is also present in humans, the contexts where this could be relevant to human susceptibility to liver injury remain to be determined. However, since sustained JNK activation accompanies most acute and chronic liver disease and since sustained JNK activation depends on the level of SAB expression, the SAB-dependent activation loop represents a potentially relevant therapeutic target to explore.

Lipoapoptosis may be one particularly translatable example. Lipotoxicity also is dependent on sustained JNK activation and SAB (13). We found resistance to palmitic acid

toxicity in females PMH of females versus males which may be relevant to the progression of NASH. However, future studies will be needed to determine if the ERα-p53-*miR34a-5p*-SAB repression pathway contributes to the recently recognized resistance of premenopausal human females to NASH (6, 66-70). Since premenopausal human females exhibit decreased susceptibility to non-alcoholic steatohepatitis and fibrosis which is no longer the case in postmenopause, it is interesting to speculate that the postmenopausal increase in SAB levels may contribute to the pathogenesis of NASH. Furthermore the postmenopausal increase in SAB levels further supports the role of estrogen in repression of SAB. In addition, *miR34a* can be regulated by IRE-1α mediated RIDD activation or inactivation which may play a role in expression of caspase2 or SIRT1 (both targets of *miR34a*) depending on the context during the progression of NASH (71, 72).

Since *miR34a-5p* has other targets besides SAB, as noted above, it remains possible that their repression also contributes to resistance to acute liver injury. SIRT1 in particular is a potentially relevant target as it deacetylates and partially inhibits p53. A possible positive feedback effect of increased *miR34a* to increase p53 expression and to increase p53 activity (acetyl-p53) by repressing SIRT1 expression is plausible. Liver specific *Sirt1* knockout has been reported to protect against LPS-galactosamine toxicity (73). In addition, in PMH, *Sirt1* deletion, causing increased acetylation and activity of p53, protected against ActD/TNF induced apoptosis. In contrast, *Sirt1* transgenic mice exhibited protection from APAP toxicity (74) and induction of *Sirt1* knockdown has been shown to worsen APAP toxicity (75). In addition, treatment with a SIRT1 activator has been shown to have no effect on early injury (6 hours) after APAP but decreases late injury (24hours), while enhancing mitochondrial biogenesis and

liver regeneration. Furthermore, Resveratrol, which activates SIRT1, protected against APAP liver injury (76, 77). Taken together, conflicting evidence exists on the role of SIRT1 in acute injury models. However, we observed that basal SIRT1 levels were actually higher in female mouse and human livers and *miR34a*$^{i\Delta Hep}$ mice exhibited no change in SIRT1. This argues against an important role of SIRT1 repression in determining the sex difference in acute liver injury models. Therefore, the findings overall support the conclusion that repression of SAB expression by *miR34a* is the major determinant of resistance to liver injury in female mice.

One additional caveat that should be discussed is that GSH recovery is faster in APAP-treated females than males. Therefore, the question is if the faster GSH recovery dampens sustained JNK activation and protects or if decreased JNK activation is a consequence of less toxicity in females. We showed that there is no intrinsic sex difference in GSH recovery in response to nontoxic phorone induced depletion. Furthermore, GCLC, the catalytic subunit of GCL, actually rapidly declines in APAP treated males, possibly due to degradation, even before cell death begins in males and correlates with sustained JNK activation. In contrast, GCLC protein does not increase or decrease in females. Furthermore, in males treated with *miR34a-5p* mimic which decreases SAB protein levels, the recovery of GSH is accelerated similar to wild type females. Conversely, *miR34a* deletion in females which express increased SAB lead to impaired GSH recovery comparable to wild type males. Therefore, we conclude that GSH recovery rate mainly reflects the severity of JNK activation and liver injury and is not the mechanism for sex difference in APAP toxicity.

In conclusion, the level of SAB expression in mitochondria plays a pivotal role in acute liver injury by mediating the extent of sustained activation of JNK. Graded increased expression

of SAB in *Sab*$^{i\Delta Hep}$ mice has revealed a direct correlation between the level of SAB expression and the extent of liver injury. The interaction of JNK with SAB is required for this effect of SAB and SAB is required to sustain this activation. Females express markedly lower levels of SAB accounting for resistance to acute injury in different liver injury models. SAB expression is low in females due to an ERα → ↑p53 → ↑*miR34a-5p* → ↓SAB pathway in which the translation of *Sab* mRNA is presumably inhibited by targeting of the coding region by *miR34a-5p* (Figure 7E). In support of the importance of the level of SAB expression as a determinant of liver injury, activation of ERα in males increased p53 and *miR34a-5p* which repressed SAB expression and protected from liver injury. Conversely, inhibition of ERα in female mice decreased p53 and *miR34a-5p* levels which increased SAB expression, overcoming the female resistance to acute liver injury. In future studies it will be of great interest to examine if the sex difference seen in hepatic SAB is present in nonhepatic tissues and to identify the role of SAB in extrahepatic organ injury.

METHODS

Mice

Male and female C57BL/6NHsd mice (6–8 weeks of age) were purchased from Envigo and bred to obtain littermates. 10-12 weeks old cage mate littermates were used for experiments. *Jnk1*$^{f/f}$ and *Jnk2*$^{f/f}$ (C57BL/6J strain) mice were generated by Dr. Roger Davis, as described previously [6]. *Jnk1*$^{f/f}$ and *Jnk2*$^{f/f}$ mice were cross bred to obtain *Jnk1/2*$^{f/f}$ littermates. *Sab*$^{f/f}$ mice (C57BL/6NHsd strain) were generated as described before (11). *Sab*$^{f/f}$ mice were crossbred with Alb-Cre^{ERT2} mice (Alb$^{tm1(cre/ERT2)Mtz}$), kindly provided by Dr. Pierre Chambon (Institut de Genetique et de Biologie Moleculaire et Cellulaire, France) to generate tamoxifen-inducible hepatocyte-specific *Sab* KO mice (*Sab*$^{i\Delta Hep}$) (11). Mice were crossbred with *Sab*$^{f/f}$ mice more than 20 generations. *miR34a*$^{f/+}$ and *miR34a*$^{+/+}$ littermates were purchased from Jackson laboratory and bred to obtain *miR34a*$^{f/f}$ mice (C57BL/6J strain). Inducible hepatocyte-specific KO *Jnk1/2*$^{i\Delta Hep}$ or *miR34a*$^{i\Delta Hep}$ mice were obtained by tail vein injection of AAV8-TBG-CRE (purchased from UPenn) to *Jnk1/2*$^{f/f}$ or *miR34a*$^{f/f}$ mice respectively. All experiments were performed using cage mate littermates. In all experiments the substrain background of mice was carefully controlled.

Human liver tissue biopsy samples

Human liver biopsy tissues were obtained from the Duke University Health Systems (DUHS) NAFLD Clinical Database. The DUHS NAFLD Clinical Database, established in 2007, is a prospective, open-enrolling and well-annotated clinical database of patients who underwent clinical and histological evaluations of the suspected diagnosis of NAFLD. The DUHS NAFLD

Clinical Database was approved by the Duke University Institutional Review Board and was performed in accordance with the Declaration of Helsinki ethical guidelines. Details of the DUHS NAFLD clinical database are described in the previous publication (78). The database is also linked to tissue repositories in which biosamples (e.g., blood, liver tissues) were collected at the time of the percutaneous liver biopsies or intraoperative needle liver biopsies in case a patient received bariatric surgery. All the participants provided written informed consent prior to the study enrollment.

Cases with normal or minimal non-specific histologic changes were identified in the database. The diagnosis of diabetes mellitus, bariatric surgery, and post-liver transplant were excluded from the case selection. Menopausal status was defined as natural cessation of menstruation (no menstruation for more than 12 months) or a history of bilateral oophorectomy, using self-reported information collected via a standardized research questionnaire as a part of the DUHS NAFLD Clinical Database study. The menopausal status was then confirmed by serum FSH. Female cases with oral contraceptive or hormone replacement therapy were excluded. After the exclusion, five pre-menopausal women, three post-menopausal women, and eight age-/ BMI-matched men were randomly selected. Age/BMI differences for female-male pairs were 2.6 ± 1.9 (range: 0-6 years) and 2.6 ± 1.4 km/m2 (range: 0.36-4.49 km/m2). Statistical analysis of SAB expression of female-male pairs was performed using paired 2-tailed Student's *t*-test. $P < 0.05$ is statistically significant.

AAV and adenoviral vectors

Ad-lacZ and Ad-*SAB* were generated using ViraPower Adenoviral Gateway Expression kit (invitrogen) as described before (10, 79). Adenoviral vectors with CMV promotor were purified

and concentrated using Vivapure Adeno-PACK (Sartorius Stedim Biotech S.A.). Adenoviral titer was determined by infection of viral vector into HEK293 cells (Invitrogen) and staining of infected cells with adenoviral hexon antiserum (Santa Cruz Biotechnology). Different doses of adenoviral vectors were injected in male mice weighing 20g through tail vein and experiments were performed 10-14 days later. AAV8-TBG-GFP and AAV8-TBG-Cre were purchased from Penn Vector Core/Addgene. $\geq 2x10^{12}$ viral gene copy (GC) was injected to ≤ 20g mice through tail vein. Two weeks later experiments were performed. For some experiments, AAV8-TBG-CRE and Ad-*SAB* ($0.5x10^{9}$i.u) were injected simultaneously. Ad-miR-GFP and Ad-*miR34a-5p* mimic were purchased from Applied Biological Materials (abm) Inc and amplified, purified and concentrated in our lab.

In vivo treatment with ERα agonist and ERα/β antagonist

Mice received ERα agonist PPT 5 mg/kg/dose/day in EtOH/Corn Oil subcutaneously for 5 days per week for 2 weeks. In vivo experiments and PMH isolation were performed on next day after PPT treatment. Mice received ERα/β antagonist fulvestrant 2 or 5 mg/kg in EtOH/Corn Oil subcutaneously (1 dose per week for 3 weeks). Adenoviral vector injection was performed 2-3 days after the first dose of fulvestrant. PPT or fulvestrant was first dissolved in ethanol and diluted in corn oil (1:9 ratio), and control animals received vehicle as described (80, 81).

smallRNA sequence analysis

Liver from 12 weeks old chow fed C57BL/6N male and female littermates were snap frozen in RNA*later* RNA stabilizing solution. miRNA was isolated using Qiagen miRNA extraction kit and miRNA library was performed using QIAseq miRNA library kit. Next-generation sequencing

(NGS) was performed using illumina 1x75HT 30GB. Mature miRNAseq analysis was performed on three independent libraries prepared from normal liver of three individual male and female C57BL/6N littermates. miRNA-seq data was analyzed using Partek Flow version 5 (Partek Inc., St. Louis, MO). Raw sequencing reads were first trimmed for adapters and then for quality score (base positions with Phred score less than 20 were trimmed from both ends, and trimmed reads shorter than 15 nt were excluded from downstream analyses). Trimmed reads were mapped to the mouse genome mm10 using Bowtie (seed mismatch limit 1 and seed length 10). Aligned reads were then quantified to mirBase mature miRNAs v21 using Partek E/M method. Finally, miRNAs with 5 raw read counts in at least one sample were normalized using Upper Quartile normalization (82) with offset 1 and analyzed for differential expression using Partek Gene Specific Analysis method. The differentially expressed miRNA lists (GEO accession number "GSE135299") were generated for each comparison using cutoffs FDR<0.05 and fold changes greater than 1.5 in either direction. The *p* values are calculated based on a Student's t-test of the replicate normalized miRNA expression values for each miRNA in the female versus male groups. *p* values less than 0.05 are indicated as significant change.

Statistics

A minimum of three biological replicates were considered for all studies. Data are expressed as mean ± SD or SEM. Statistical analyses were performed using the unpaired or paired 2-tailed Student's t-test. Multivariate data were analyzed by 1-way ANOVA with Bonferroni correction. $P < 0.05$ is statistically significant.

Study approval

Animal breeding and experiments were performed as approved by Institutional Animal Care and Utilization Committee (IACUC) and Institutional Biosafety Committee (IBC). All animals received care under the institutional guidelines. Human liver tissue biopsy and blood samples were used as approved by the Duke University Institutional Review Board and University of Southern California Institutional Review Board.

AUTHOR CONTRIBUTIONS

S.W, R.W.M.M, C.C, J.Z, F.W.M.A and T.A.T executed all experiments. Y.C, M.L, S.W and T.A.T analyzed miRNAseq data. A.S, M.F.A, Y.W and A.M.D provided human liver samples. M.A provided by ASO and GalNAc-ASO. R.D provided *Jnk*$1^{f/f}$ and *Jnk*$2^{f/f}$ mice. N.K, T.A.T and S.W designed experiments and wrote manuscript and all authors read and provided input into the final manuscript. S.W and R.W.M.M are co-first authors. Additionally S.W contributed with Institutional funding.

ACKNOWLEDGMENTS

This research was supported by R01DK067215 (N.K), RO1DK107220 (R.D), the Donald E. and Delia Baxter Foundation Faculty Fellows award (S.W.), the USC Research Center for Liver Diseases Pilot Project award (S.W) and the USC Research Center for Liver Disease's Cell Separation and Culture, Cell and Tissue Imaging, Histology, and Metabolic/ Analytical/ Instrumentation Cores (P30DK048522) (N.K). The Duke NAFLD Clinical Database and Biorepository was supported by the Duke University Florence McAlister Professorship and the NAFLD Clinical Research Program. The bioinformatics software and computing resources used in the analysis are funded by the USC Office of Research and the Norris Medical Library of USC.

ABBREVIATIONS

Acetyl-p53	Acetylated p53
ActD	Actinomycin D
ALT	Alanine aminotransferase
APAP	Acetaminophen
ASO	Antisense oligonucleotide
ATP	Adenosine triphosphate
BAX	BCL2 associated X
BCL-X_L	BCL2 like 1
BID	BH3 interacting domain death agonist
BIM	BCL2 like 11
BMS	2-Chloro-3-methyl-4-[(7R,7aS)-tetrahydro-7-hydroxy-1,3-dioxo-1H-pyrrolo[1,2-c]imidazol-2(3H)-yl]benzonitrile
DPN	Diarylpropionitrile
ER	Endoplasmic reticulum
ERα	Estrogen receptor alpha
ERβ	Estrogen receptor beta
GalN	D-Galactosamine
GCLC	Glutamate-cysteine ligase catalytic subunit
GSH	Glutathione
JNK	C-Jun-N-terminal kinase
LPS	Lipopolysaccharides
MAPK	Mitogen-activated protein kinase
MCL-1	Myeloid cell leukemia sequence 1
NAPQI	N-acetyl-p-benzoquinone imine
NASH	Nonalcoholic steatohepatitis
OCR	Oxygen consumption rate
PMH	Primary mouse hepatocyte
PPT	Propylpyrazole triol
PTPN6	Protein tyrosine phosphatase, nonreceptor type 6
PUMA	BCL2 binding component 3
ROS	Reactive oxygen species
SAB	SH3 homology associated BTK binding protein (SH3BP5)
SRC	SRC proto-oncogene (nonreceptor tyrosine kinase)
TNF	Tumor necrosis factor

REFERENCES

1. Gunawan BK, Liu ZX, Han D, Hanawa N, Gaarde WA, Kaplowitz N. c-Jun N-terminal kinase plays a major role in murine acetaminophen hepatotoxicity. *Gastroenterology.* 2006;131(1):165-178.
2. Hanawa N, Shinohara M, Saberi B, Gaarde WA, Han D, Kaplowitz N. Role of JNK translocation to mitochondria leading to inhibition of mitochondria bioenergetics in acetaminophen-induced liver injury. *J Biol Chem.* 2008;283(20):13565-13577.
3. Zhang J, et al. The role of MAP2 kinases and p38 kinase in acute murine liver injury models. *Cell Death Dis.* 2017;8(6):e2903.
4. Sharma M, Gadang V, Jaeschke A. Critical role for mixed-lineage kinase 3 in acetaminophen-induced hepatotoxicity. *Mol Pharmacol.* 2012;82(5):1001-1007.
5. Nakagawa H, et al. Deletion of apoptosis signal-regulating kinase 1 attenuates acetaminophen-induced liver injury by inhibiting c-Jun N-terminal kinase activation. *Gastroenterology.* 2008;135(4):1311-1321.
6. Vernia S, et al. The PPARα-FGF21 hormone axis contributes to metabolic regulation by the hepatic JNK signaling pathway. *Cell Metab.* 2014;20(3):512-525.
7. Czaja MJ. JNK regulation of hepatic manifestations of the metabolic syndrome. *Trends Endocrinol Metab.* 2010;21(12):707-713.
8. Du K, Xie Y, McGill MR, Jaeschke H. Pathophysiological significance of c-jun N-terminal kinase in acetaminophen hepatotoxicity. *Expert Opin Drug Metab Toxicol.* 2015;11(11):1769-1779.
9. Win S, Than TA, Zhang J, Oo C, Min RWM, Kaplowitz N. New insights into the role and

mechanism of c-Jun-N-terminal kinase signaling in the pathobiology of liver diseases. *Hepatology.* 2018;67(5):2013-2024.

10. Win S, Than TA, Han D, Petrovic LM, Kaplowitz N. c-Jun N-terminal kinase (JNK)-dependent acute liver injury from acetaminophen or tumor necrosis factor (TNF) requires mitochondrial Sab protein expression in mice. *J Biol Chem.* 2011;286(40):35071-35078.
11. Win S, Than TA, Min RW, Aghajan M, Kaplowitz N. c-Jun N-terminal kinase mediates mouse liver injury through a novel Sab (SH3BP5)-dependent pathway leading to inactivation of intramitochondrial Src. *Hepatology.* 2016;63(6):1987-2003.
12. Win S, Than TA, Fernandez-Checa JC, Kaplowitz N. JNK interaction with Sab mediates ER stress induced inhibition of mitochondrial respiration and cell death. *Cell Death Dis.* 2014;5:e989.
13. Win S, Than TA, Le BH, García-Ruiz C, Fernandez-Checa JC, Kaplowitz N. Sab (Sh3bp5) dependence of JNK mediated inhibition of mitochondrial respiration in palmitic acid induced hepatocyte lipotoxicity. *J Hepatol.* 2015;62(6):1367-1374.
14. Chambers JW, LoGrasso PV. Mitochondrial c-Jun N-terminal kinase (JNK) signaling initiates physiological changes resulting in amplification of reactive oxygen species generation. *J Biol Chem.* 2011;286:16052-16062.
15. Dai G, He L, Chou N, Wan YJ. Acetaminophen metabolism does not contribute to gender difference in its hepatotoxicity in mouse. *Toxicol Sci.* 2006;92(1):33-41.
16. Rohrer PR, Rudraiah S, Goedken MJ, Manautou JE. Is nuclear factor erythroid 2-related factor 2 responsible for sex differences in susceptibility to acetaminophen-induced hepatotoxicity in mice? *Drug Metab Dispos.* 2014;42(10):1663-1674.

17. Du K, Williams CD, McGill MR, Jaeschke H. Lower susceptibility of female mice to acetaminophen hepatotoxicity: Role of mitochondrial glutathione, oxidant stress and c-jun N-terminal kinase. *Toxicol Appl Pharmacol.* 2014;281(1):58-66.

18. Kaplowitz N. Idiosyncratic drug hepatotoxicity. *Nat Rev Drug Discov.* 2005;4(6):489-499.

19. Saito C, Lemasters JJ, Jaeschke H. c-Jun N-terminal kinase modulates oxidant stress and peroxynitrite formation independent of inducible nitric oxide synthase in acetaminophen hepatotoxicity. *Toxicol Appl Pharmacol.* 2010;246(1-2):8-17.

20. Jaeschke H, Gores GJ, Cederbaum AI, Hinson JA, Pessayre D, Lemasters JJ. Mechanisms of hepatotoxicity. *Toxicol Sci.* 2002;65(2):166-176.

21. Deng Y, Ren X, Yang L, Lin Y, Wu X. A JNK-dependent pathway is required for TNFalpha-induced apoptosis. *Cell.* 2003;115(1):61-70.

22. Putcha GV, et al. JNK-mediated BIM phosphorylation potentiates BAX-dependent apoptosis. *Neuron.* 2003;38(6):899-914.

23. Fan M, Goodwin M, Vu T, Brantley-Finley C, Gaarde WA, Chambers TC. Vinblastine-induced phosphorylation of Bcl-2 and Bcl-XL is mediated by JNK and occurs in parallel with inactivation of the Raf-1/MEK/ERK cascade. *J Biol Chem.* 2000;275(39):29980-29985.

24. Inoshita S, et al. Phosphorylation and inactivation of myeloid cell leukemia 1 by JNK in response to oxidative stress. *J Biol Chem.* 2002;277(46):43730-43734.

25. Chen D, et al. p53 Up-regulated Modulator of Apoptosis Induction Mediates Acetaminophen-Induced Necrosis and Liver Injury in Mice. *Hepatology.* 2019;69(5):2164-2179.

26. Dhanasekaran DN, Reddy EP. JNK-signaling: A multiplexing hub in programmed cell death. *Genes Cancer.* 2017;8(9-10):682-694.

27. Bourdi M, Davies JS, Pohl LR. Mispairing C57BL/6 substrains of genetically engineered mice and wild-type controls can lead to confounding results as it did in studies of JNK2 in acetaminophen and concanavalin A liver injury. *Chem Res Toxicol.* 2011;24(6):794-796.

28. Duan L, et al. Differential susceptibility to acetaminophen-induced liver injury in sub-strains of C57BL/6 mice: 6N versus 6J. *Food Chem Toxicol.* 2016;98(Pt B):107-118.

29. Shinohara M, et al. Silencing glycogen synthase kinase-3beta inhibits acetaminophen hepatotoxicity and attenuates JNK activation and loss of glutamate cysteine ligase and myeloid cell leukemia sequence 1. *J Biol Chem.* 2010;285(11):8244-8255.

30. Hewitt SC, Korach KS. Estrogen Receptors: New Directions in the New Millennium. *Endocr Rev.* 2018;39(5):664-675.

31. Chow JD, Jones ME, Prelle K, Simpson ER, Boon WC. A selective estrogen receptor α agonist ameliorates hepatic steatosis in the male aromatase knockout mouse. *J Endocrinol.* 2011;210(3):323-334.

32. Kuiper GG, et al. Comparison of the ligand binding specificity and transcript tissue distribution of estrogen receptors alpha and beta. *Endocrinology.* 1997;138(3):863-870.

33. Mårtensson UE, et al. Deletion of the G protein-coupled receptor 30 impairs glucose tolerance, reduces bone growth, increases blood pressure, and eliminates estradiol-stimulated insulin release in female mice. *Endocrinology.* 2009;150(2):687-698.

34. Osborne CK, Wakeling A, Nicholson RI. Fulvestrant: an oestrogen receptor antagonist with a novel mechanism of action. *Br J Cancer.* 2004;90 Suppl 1:S2-6.

35. Lai AC, Crews CM. Induced protein degradation: an emerging drug discovery paradigm. *Nat Rev Drug Discov.* 2017;16(2):101-114.

36. Kraichely DM, Sun J, Katzenellenbogen JA, Katzenellenbogen BS. Conformational changes and coactivator recruitment by novel ligands for estrogen receptor-alpha and estrogen receptor-beta: correlations with biological character and distinct differences among SRC coactivator family members. *Endocrinology.* 2000;141(10):3534-3545.

37. Petrie WK, et al. G protein-coupled estrogen receptor-selective ligands modulate endometrial tumor growth. *Obstet Gynecol Int.* 2013;2013:472720.

38. Berger C, Qian Y, Chen X. The p53-estrogen receptor loop in cancer. *Curr Mol Med.* 2013;13(8):1229-1240.

39. Ito A, et al. p300/CBP-mediated p53 acetylation is commonly induced by p53-activating agents and inhibited by MDM2. *EMBO J.* 2001;20(6):1331-1340.

40. Lee TK, Lau TC, Ng IO. Doxorubicin-induced apoptosis and chemosensitivity in hepatoma cell lines. *Cancer Chemother Pharmacol.* 2002;49(1):78-86.

41. Seitz SJ, et al. Chemotherapy-induced apoptosis in hepatocellular carcinoma involves the p53 family and is mediated via the extrinsic and the intrinsic pathway. *Int J Cancer.* 2010;126(9):2049-2066.

42. Yamakuchi M, Ferlito M, Lowenstein CJ. miR-34a repression of SIRT1 regulates apoptosis. *Proc Natl Acad Sci U S A.* 2008;105(36):13421-13426.

43. Vaziri H, et al. hSIR2(SIRT1) functions as an NAD-dependent p53 deacetylase. *Cell.* 2001;107(2):149-159.

44. Zhao Y, et al. Acetylation of p53 at lysine 373/382 by the histone deacetylase inhibitor depsipeptide induces expression of p21(Waf1/Cip1). *Mol Cell Biol.* 2006;26(7):2782-2790.

45. Huo Y, et al. Protective role of p53 in acetaminophen hepatotoxicity. *Free Radic Biol Med.*

2017;106:111-117.

46. Navarro F, Lieberman J. miR-34 and p53: New Insights into a Complex Functional Relationship. *PLoS One.* 2015;10(7):e0132767.

47. Graham MJ, et al. Cardiovascular and Metabolic Effects of ANGPTL3 Antisense Oligonucleotides. *N Engl J Med.* 2017;377(3):222-232.

48. Cazanave SC, et al. JNK1-dependent PUMA expression contributes to hepatocyte lipoapoptosis. *J Biol Chem.* 2009;284(39):26591-26602.

49. Wiltshire C, Matsushita M, Tsukada S, Gillespie DA, May GH. A new c-Jun N-terminal kinase (JNK)-interacting protein, Sab (SH3BP5), associates with mitochondria. *Biochem J.* 2002;367(Pt 3):577-585.

50. Cubero FJ, et al. Combined Activities of JNK1 and JNK2 in Hepatocytes Protect Against Toxic Liver Injury. *Gastroenterology.* 2016;150(4):968-981.

51. Zoubek ME, et al. Protective role of c-Jun N-terminal kinase-2 (JNK2) in ibuprofen-induced acute liver injury. *J Pathol.* 2019;247(1):110-122.

52. Chambers TP, Santiesteban L, Gomez D, Chambers JW. Sab mediates mitochondrial dysfunction involved in imatinib mesylate-induced cardiotoxicity. *Toxicology.* 2017;382:24-35.

53. Chambers TP, Portalatin GM, Paudel I, Robbins CJ, Chambers JW. Sub-chronic administration of LY294002 sensitizes cervical cancer cells to chemotherapy by enhancing mitochondrial JNK signaling. *Biochem Biophys Res Commun.* 2015;463:538-544.

54. Paudel I, Hernandez SM, Portalatin GM, Chambers TP, Chambers JW. Sab concentrations indicate chemotherapeutic susceptibility in ovarian cancer cell lines. *Biochem J.* 2018;475:3471-3492.

55. Chang TC, et al. Transactivation of miR-34a by p53 broadly influences gene expression and promotes apoptosis. *Mol Cell.* 2007;26(5):745-752.

56. Li XJ, Ren ZJ, Tang JH. MicroRNA-34a: a potential therapeutic target in human cancer. *Cell Death Dis.* 2014;5:e1327.

57. Fuchs SY, Adler V, Pincus MR, Ronai Z. MEKK1/JNK signaling stabilizes and activates p53. *Proc Natl Acad Sci U S A.* 1998;95(18):10541-10546.

58. Shi Y, et al. ROS-dependent activation of JNK converts p53 into an efficient inhibitor of oncogenes leading to robust apoptosis. *Cell Death Differ.* 2014;21(4):612-623.

59. Saha MN, et al. Targeting p53 via JNK pathway: a novel role of RITA for apoptotic signaling in multiple myeloma. *PLoS One.* 2012;7(1):e30215.

60. Mennecozzi M, Landesmann B, Palosaari T, Harris G, Whelan M. Sex differences in liver toxicity-do female and male human primary hepatocytes react differently to toxicants in vitro? *PLoS One.* 2015;10:e0122786.

61. Fontana RJ. Acute liver failure including acetaminophen overdose. *Med Clin North Am.* 2008;92(4):761-794.

62. Rubin JB, Hameed B, Gottfried M, Lee WM, Sarkar M; Acute Liver Failure Study Group. Acetaminophen-induced Acute Liver Failure Is More Common and More Severe in Women. *Clin Gastroenterol Hepatol.* 2018;16(6):936-946.

63. McCully JD, Toyoda Y, Wakiyama H, Rousou AJ, Parker RA, Levitsky S. Age- and gender-related differences in ischemia/reperfusion injury and cardioprotection: effects of diazoxide. *Ann Thorac Surg.* 2006;82(1):117-123.

64. Murphy E, Steenbergen C. Gender-based differences in mechanisms of protection in

myocardial ischemia-reperfusion injury. *Cardiovasc Res.* 2007;75(3):478-486.

65. Chu AS, Chopra KB, Perlmutter DH. Is severe progressive liver disease caused by alpha-1-antitrypsin deficiency more common in children or adults? *Liver Transpl.* 2016;22(7):886-894.

66. Suzuki A. NASH in Special Populations. *Gastroenterol Hepatol (N Y).* 2014;10(4):262-264.

67. Yang JD, et al. Gender and menopause impact severity of fibrosis among patients with nonalcoholic steatohepatitis. *Hepatology.* 2014;59(4):1406-1414.

68. Klair JS, et al; Nonalcoholic Steatohepatitis Clinical Research Network. A longer duration of estrogen deficiency increases fibrosis risk among postmenopausal women with nonalcoholic fatty liver disease. *Hepatology.* 2016;64(1):85-91.

69. Ballestri S, Nascimbeni F, Baldelli E, Marrazzo A, Romagnoli D, Lonardo A. NAFLD as a Sexual Dimorphic Disease: Role of Gender and Reproductive Status in the Development and Progression of Nonalcoholic Fatty Liver Disease and Inherent Cardiovascular Risk. *Adv Ther.* 2017;34(6):1291-1326.

70. Lonardo A, et al. Sex Differences in NAFLD: State of the Art and Identification of Research Gaps. [published online ahead of print March 29, 2019]. *Hepatology.* doi: 10.1002/hep.30626.

71. Upton JP, et al. IRE1α cleaves select microRNAs during ER stress to derepress translation of proapoptotic Caspase-2. *Science.* 2012;338(6108):818-822.

72. Yamakuchi M. MicroRNA Regulation of SIRT1. *Front Physiol.* 2012;3:68.

73. Cui X, et al. Inactivation of Sirt1 in mouse livers protects against endotoxemic liver injury by acetylating and activating NF-κB. *Cell Death Dis.* 2016;7(10):e2403.

74. Rada P, et al. SIRT1 Controls Acetaminophen Hepatotoxicity by Modulating Inflammation and

Oxidative Stress. *Antioxid Redox Signal.* 2018;28(13):1187-1208.

75. Liu X, et al. Acetaminophen Responsive miR-19b Modulates SIRT1/Nrf2 Signaling Pathway in Drug-Induced Hepatotoxicity. *Toxicol Sci.* 2019;170(2):476-488.

76. Wang Y, et al. Hepato-protective effect of resveratrol against acetaminophen-induced liver injury is associated with inhibition of CYP-mediated bioactivation and regulation of SIRT1-p53 signaling pathways. *Toxicol Lett.* 2015;236(2):82-89.

77. Wojnarová L, Kutinová Canová N, Farghali H, Kučera T. Sirtuin 1 modulation in rat model of acetaminophen-induced hepatotoxicity. *Physiol Res.* 2015;64(Suppl 4):S477-487.

78. Youssef NA, et al. Associations of depression, anxiety and antidepressants with histological severity of nonalcoholic fatty liver disease. *Liver Int.* 2013;33(7):1062-1070.

79. Than TA, Lou H, Ji C, Win S, Kaplowitz N. Role of cAMP-responsive element-binding protein (CREB)-regulated transcription coactivator 3 (CRTC3) in the initiation of mitochondrial biogenesis and stress response in liver cells. *J Biol Chem.* 2011;286(25):22047-22054.

80. Miller NR, Jover T, Cohen HW, Zukin RS, Etgen AM. Estrogen can act via estrogen receptor alpha and beta to protect hippocampal neurons against global ischemia-induced cell death. *Endocrinology.* 2005;146(7):3070-3079.

81. Ariazi EA, et al. Emerging principles for the development of resistance to antihormonal therapy: implications for the clinical utility of fulvestrant. *J Steroid Biochem Mol Biol.* 2006;102(1-5):128-138.

82. Bullard JH, Purdom E, Hansen KD, Dudoit S. Evaluation of statistical methods for normalization and differential expression in mRNA-Seq experiments. *BMC Bioinformatics.* 2010;11:94.

Figure 1

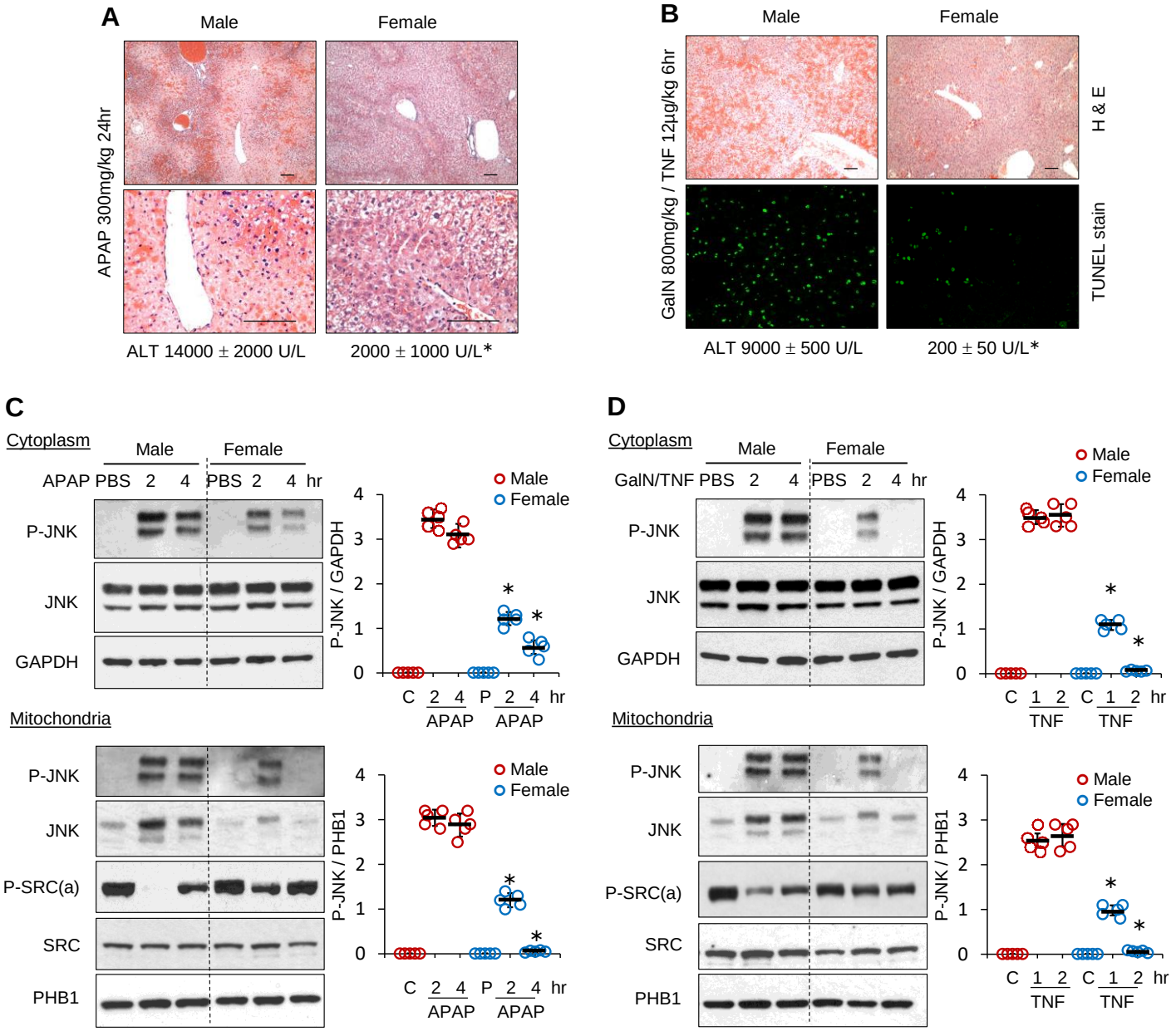
A
Male
Female
APAP 300mg/kg 24hr
ALT 14000 ± 2000 U/L
2000 ± 1000 U/L*
B
Male
Female
GalN 800mg/kg / TNF 12μg/kg 6hr
H & E
TUNEL stain
ALT 9000 ± 500 U/L
200 ± 50 U/L*
C
Cytoplasm
Male
Female
APAP PBS 2 4 PBS 2 4 hr
P-JNK
JNK
GAPDH
P-JNK / GAPDH
Male
Female
C 2 4 P 2 4 hr
APAP APAP
Mitochondria
P-JNK
JNK
P-SRC(a)
SRC
PHB1
P-JNK / PHB1
D
Cytoplasm
GalN/TNF PBS 2 4 PBS 2 4 hr
C 1 2 C 1 2 hr
TNF TNF
Mitochondria

Figure 1. Sex difference in APAP induced necrotic or GalN/TNF induced apoptotic liver injury. **(A, B**) Ten to twelve weeks old C57BL/6N wild type male and female littermates were fasted overnight and treated. ALT and H&E staining were examined 24hr after APAP 300mg/kg treatment. ALT, H&E and TUNEL staining were examined 6hr after GalN 800mg/kg/TNF 12μg/kg treatment. Original magnification: x10 and 40. Scale bars: 100μm. N=5 mice in each group. (∗) = P<0.05 vs male, by unpaired, 2-tailed Student's *t* test. Data are presented as the mean ± SD. **(C)** Liver cytoplasm and mitochondria from male and female littermates were isolated by differential centrifugation after PBS or 2, 4 hr after APAP treatment or **(D)** GalN/PBS [C] or GalN/TNF 1, 2 hr treatment. 30μg of protein extract from cytoplasm or mitochondria was loaded for immuno blot using anti-P-JNK, JNK, P-SRC (active), c-SRC. GAPDH (cytoplasm) and PHB1 (mitochondria) were used as loading controls. Representative immunoblot of 3 separate experiments. N=5 mice in each group. Dot plot graph: (∗) = P<0.05 vs male, by 1-way ANOVA with Bonferroni correction. Data are presented as the mean ± SEM.

Figure 2

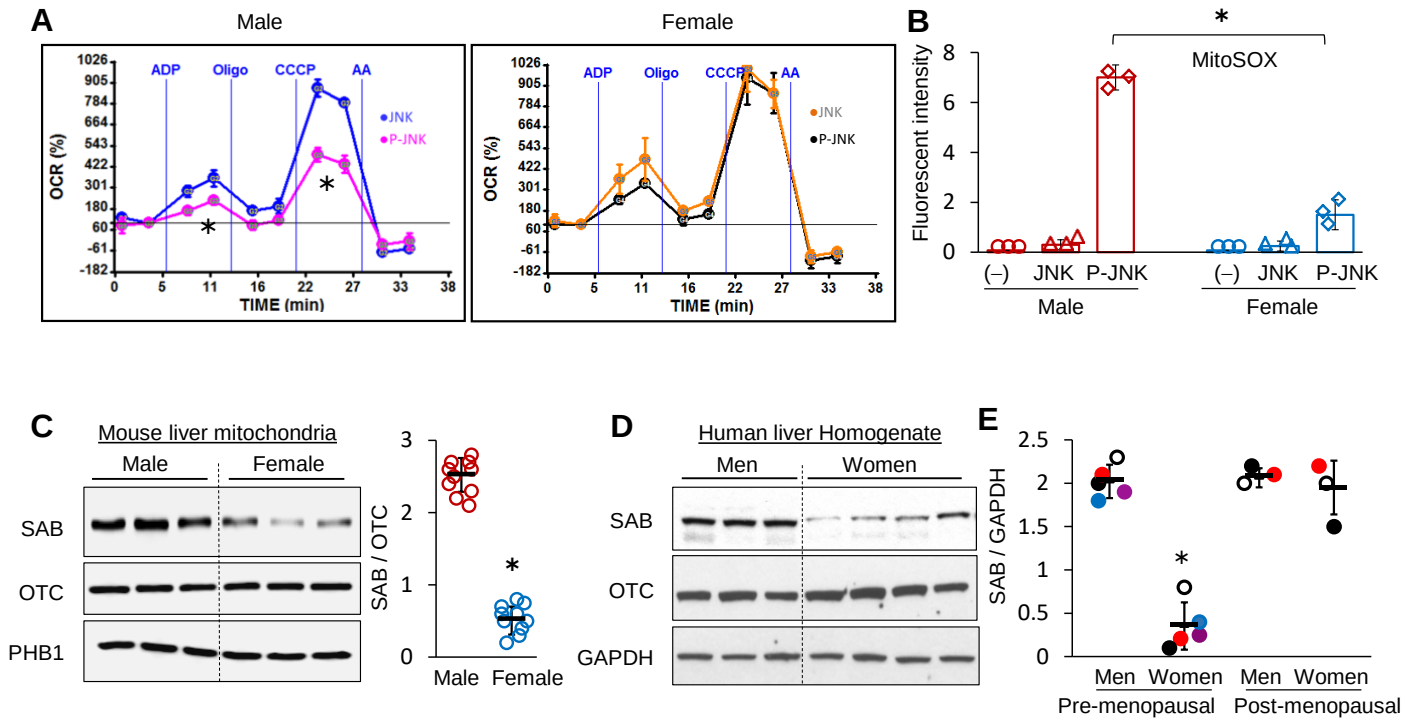
A
Male
Female
ADP
Oligo
CCCP
AA
JNK
P-JNK
OCR (%)
TIME (min)
B
MitoSOX
Fluorescent intensity
(–)
JNK
P-JNK
Male
Female
C
Mouse liver mitochondria
Male
Female
SAB
OTC
PHB1
SAB / OTC
D
Human liver Homogenate
Men
Women
SAB
OTC
GAPDH
E
SAB / GAPDH
Men
Women
Pre-menopausal
Post-menopausal

Figure 2. Sex difference in P-JNK inhibition of mitochondrial respiration and SAB expression. **(A)** Isolated mitochondria from male or female littermates were incubated with ATP plus recombinant JNK (1+2) or P-JNK (1+2) and then ADP, oligomycin, CCCP, or antimycin A were injected sequentially and OCR measured to determine state3 and maximal respiration in Seahorse XF analyzer. Representative trace of 5 separate experiments. (∗) = P<0.05 vs JNK, by 1-way ANOVA with Bonferroni correction. Data are presented as the mean ± SD of multiple wells of each treatment. **(B)** Mitochondria were isolated as for mitochondrial respiration assay. Mitochondria were pre-incubated with MitoSox and then treated with JNK or P-JNK with ATP and fluorescence intensity was measured to determine superoxide production. N=3 mice in each group. (∗) = P<0.05 vs male, by paired, 2-tailed Student's *t* test. **(C)** Mitochondria from wild type male and female littermates were immunoblotted with anti-SAB, OTC or PHB1. Representative immunoblot of 3 separate experiments. N=10 mice in each group. Dot plot graph: (∗) = P<0.05 vs male, by paired, 2-tailed Student's *t* test. **(D)** SAB expression in representative human liver homogenates from premenopausal females and matched males were examined by immunoblot. (**E**) Age and BMI matched male and female were divided into pre-menopausal group or post-menopausal group according to the serum estradiol (E2) and follicular stimulating hormone (FSH) level and menstrual and gynecological history (shown in the Table S1). In each group, male and female pairs were same color symbol in figure. All liver biopsy samples were histologically classified as mild non-specific abnormalities. SAB and GAPDH were determined by western blot and densitometry. N=5 pairs in pre-menopausal group and N=3 pairs in post-menopausal group. Dot plot graph: (∗) = *P* <0.05 versus male, by paired, 2-tailed Student's t test. Data are presented as the mean ± SEM.

Figure 3

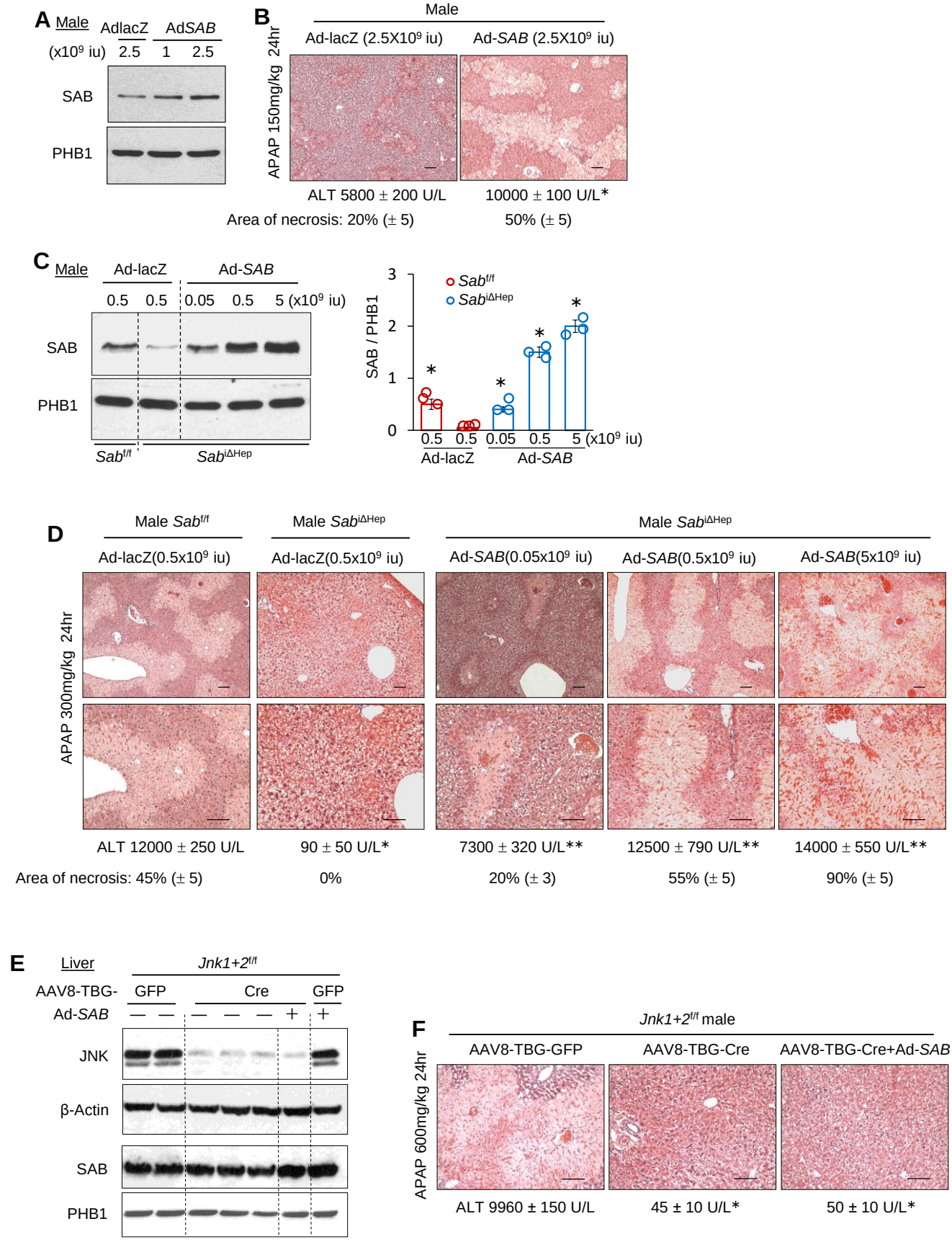
A Male
AdlacZ
AdSAB
(x10⁹ iu) 2.5 1 2.5
SAB
PHB1
B
Male
Ad-lacZ (2.5X10⁹ iu)
Ad-SAB (2.5X10⁹ iu)
APAP 150mg/kg 24hr
ALT 5800 ± 200 U/L
10000 ± 100 U/L*
Area of necrosis: 20% (± 5)
50% (± 5)
C
Male
Ad-lacZ
Ad-SAB
0.5 0.5 0.05 0.5 5 (x10⁹ iu)
SAB
PHB1
Sab f/f
Sab iΔHep
SAB / PHB1
0.5 0.5 0.05 0.5 5 (x10⁹ iu)
Ad-lacZ
Ad-SAB
D
Male Sab f/f
Male Sab iΔHep
Male Sab iΔHep
Ad-lacZ(0.5x10⁹ iu)
Ad-lacZ(0.5x10⁹ iu)
Ad-SAB(0.05x10⁹ iu)
Ad-SAB(0.5x10⁹ iu)
Ad-SAB(5x10⁹ iu)
APAP 300mg/kg 24hr
ALT 12000 ± 250 U/L
90 ± 50 U/L*
7300 ± 320 U/L**
12500 ± 790 U/L**
14000 ± 550 U/L**
Area of necrosis: 45% (± 5)
0%
20% (± 3)
55% (± 5)
90% (± 5)
E
Liver
Jnk1+2 f/f
AAV8-TBG-
GFP
Cre
GFP
Ad-SAB
JNK
β-Actin
SAB
PHB1
F
Jnk1+2 f/f male
AAV8-TBG-GFP
AAV8-TBG-Cre
AAV8-TBG-Cre+Ad-SAB
APAP 600mg/kg 24hr
ALT 9960 ± 150 U/L
45 ± 10 U/L*
50 ± 10 U/L*

Figure 3. SAB expression in male mice determines the susceptibility to APAP induced liver injury in a JNK-dependent fashion. Wild type C57BL/6N male mice received Ad-lacZ or Ad-*SAB*. **(A)** 14 days later SAB expression was examined by immunoblot and **(B)** APAP 150 mg/kg was given intraperitoneally: H&E stain and serum ALT after 24 hours. Original magnification: x10. Scale bars: 100μm. N=3 in each group. ALT: (∗) = P<0.05 vs Ad lacZ injected $Sab^{i\Delta Hep}$, by un-paired, 2-tailed Student's *t* test. Data are presented as the mean ± SD. **(C)** $Sab^{f/f}$ or $Sab^{i\Delta Hep}$ mice received 0.05~5x10^9 IU of Ad-lacZ or Ad-*SAB*. 14 days later SAB expression was determined by immunoblot. Representative immunoblot of 3 separate experiments. N=3 in each group. Dot plot graph: (∗) = P<0.05 vs $Sab^{i\Delta Hep}$ + Ad lacZ, by 1-way ANOVA with Bonferroni correction. Data are presented as the mean ± SEM. **(D)** Mice received APAP 300mg/kg intraperitoneally and 24 hours later liver sections were H&E stained and necrotic area (%) was measured. Serum ALT (±Std error) (U/L) was measured. Original magnification: x10 and 20. Scale bars: 100μm. N=3 mice per group. ALT: (∗) = P<0.05, versus Ad-lacZ injected $Sab^{f/f}$; (∗∗) = P<0.05, versus Ad-lacZ injected $Sab^{i\Delta Hep}$, by un-paired, 2-tailed Student's *t* test. Data are presented as the mean ± SD. **(E, F)** $Jnk1/2^{f/f}$ mice received AAV8-TBG-GFP (N=3) or AAV8-TBG-Cre (N=5) or AAV8-TBG-Cre + Ad-*SAB* (N=3). 14days later JNK and SAB expression were determined by immunoblot or mice were treated with APAP to examine liver injury and serum ALT. Original magnification: x20. Scale bars: 100μm. ALT: (∗) = P<0.05, versus AAV8-TBG-GFP, by un-paired, 2-tailed Student's *t* test. Data are presented as the mean ± SD.

Figure 4

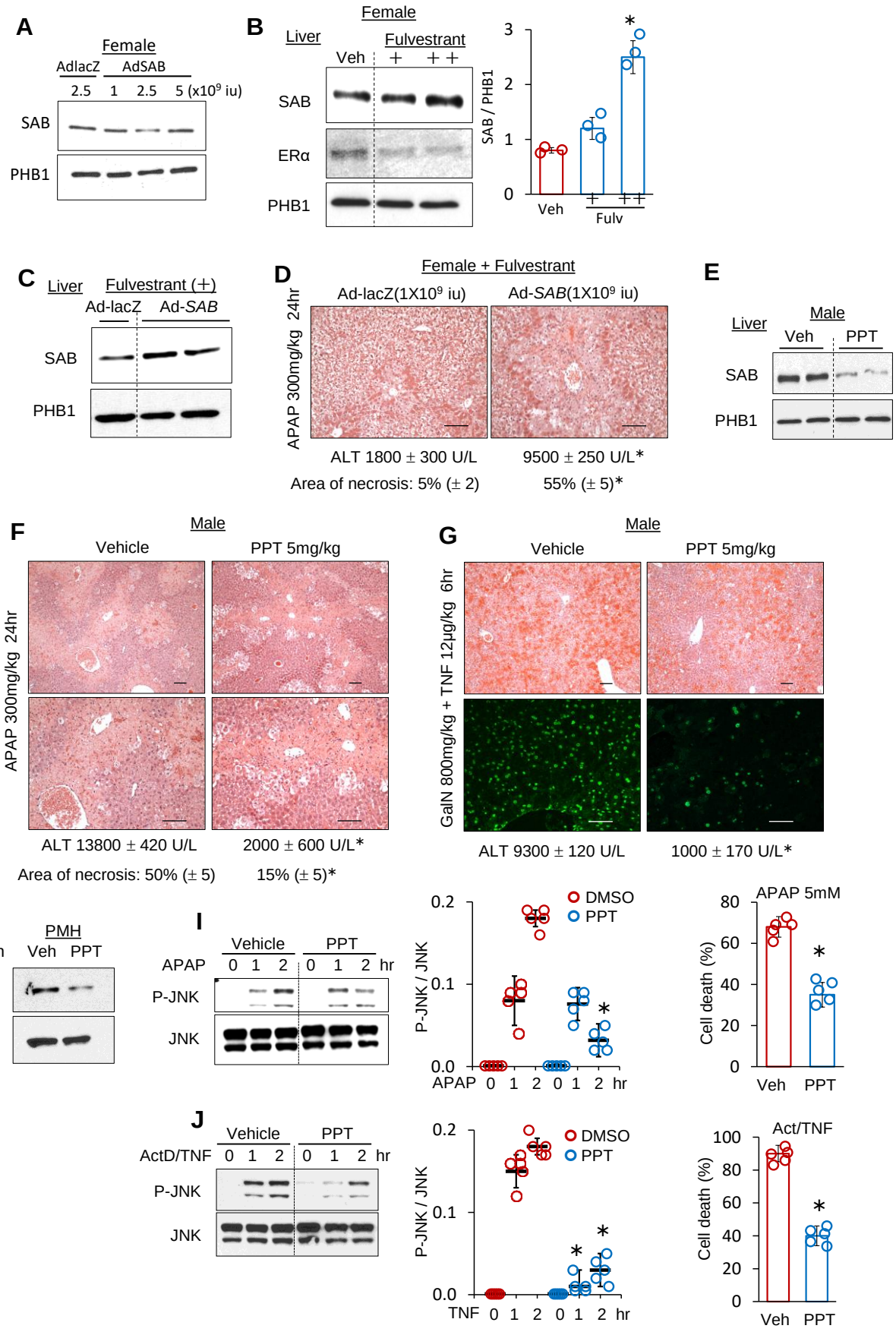
A
Female
AdlacZ
AdSAB
2.5
1
2.5
5 (x10⁹ iu)
SAB
PHB1
B
Female
Liver
Fulvestrant
Veh
+
++
SAB
ERα
PHB1
SAB / PHB1
Veh
Fulv
C
Liver
Fulvestrant (+)
Ad-lacZ
Ad-SAB
SAB
PHB1
D
Female + Fulvestrant
Ad-lacZ(1X10⁹ iu)
Ad-SAB(1X10⁹ iu)
APAP 300mg/kg 24hr
ALT 1800 ± 300 U/L
9500 ± 250 U/L*
Area of necrosis: 5% (± 2)
55% (± 5)*
E
Liver
Male
Veh
PPT
SAB
PHB1
F
Male
Vehicle
PPT 5mg/kg
APAP 300mg/kg 24hr
ALT 13800 ± 420 U/L
2000 ± 600 U/L*
Area of necrosis: 50% (± 5)
15% (± 5)*
G
Male
Vehicle
PPT 5mg/kg
GalN 800mg/kg + TNF 12μg/kg 6hr
ALT 9300 ± 120 U/L
1000 ± 170 U/L*
H
PMH
Injection
Veh
PPT
SAB
GAPDH
I
Vehicle
PPT
APAP
0 1 2 0 1 2 hr
P-JNK
JNK
DMSO
PPT
P-JNK / JNK
APAP 0 1 2 0 1 2 hr
APAP 5mM
Cell death (%)
Veh
PPT
J
Vehicle
PPT
ActD/TNF
0 1 2 0 1 2 hr
P-JNK
JNK
DMSO
PPT
P-JNK / JNK
TNF 0 1 2 0 1 2 hr
Act/TNF
Cell death (%)
Veh
PPT

Figure 4. ERα antagonist overcomes resistance to Ad-SAB expression and APAP induced liver injury in female mice. (A) Female mice received Ad-lacZ or Ad-*SAB* and examined SAB protein level. **(B)** Female mice were treated with fulvestrant (Fulv) (2 or 5 mg/kg) once per week for 3 weeks and SAB expression was determined by immunoblot. N=3 mice in each group, (∗) = P<0.05 vs vehicle, by 1-way ANOVA with Bonferroni correction. **(C)** Female littermates received total 3 doses of fulvestrant (2mg/kg) one dose before and two doses (one and two weeks) after Ad-lacZ or Ad-*SAB* ($1X10^9$ IU) tail vein injection. SAB expression in isolated mitochondria was determined by immunoblot, and **(D)** mice were treated with APAP 300mg/kg (ip). H&E and serum ALT were measured 24 hours later. Original magnification: x20. Scale bars: 100μm. N=3 mice in each group. (∗) = P<0.05, versus Ad-lacZ, by un-paired, 2-tailed Student's *t* test. **(E)** Male mice were treated with PPT for 2 weeks and mitochondria SAB level was determined, and **(F, G)** mice were treated with APAP or GalN/TNF. H&E and ALT were examined 24hr or 6hr later. Original magnification: x10 and 20. Scale bars: 100μm. N=3 mice per group. (∗) = P<0.05, versus vehicle, by un-paired, 2-tailed Student's *t* test. **(H)** Male mice were treated with PPT (5 mg/kg) or vehicle for 2 weeks and SAB expression of PMH was determined and **(I, J)** treated with APAP (5mM) or ActinmycinD (0.5μg/ml)/TNF (20ng/ml), respectively. JNK activation in whole cell lysates was determined by immunoblot using anti-P-JNK. Representative immunoblot of 3 separate experiments. (∗) = P<0.05 vs vehicle, by 1-way ANOVA with Bonferroni correction. Cell death was determined with SYTOX Green stain. N=5 experiments. (∗) = P<0.05 vs vehicle, by un-paired, 2-tailed Student's *t* test. Data are presented as the mean ± SEM.

Figure 5

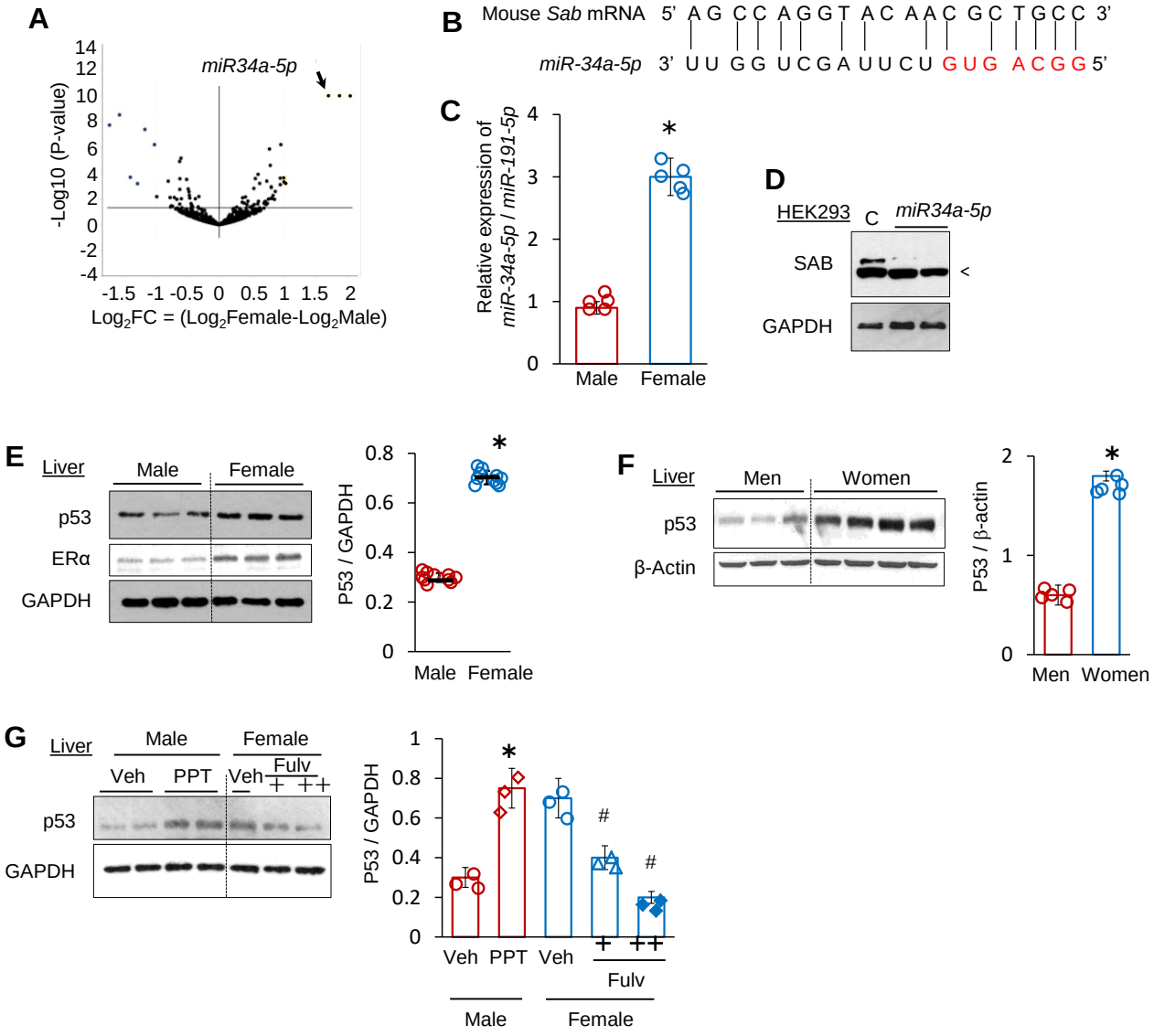
A
miR34a-5p
-Log10 (P-value)
Log2FC = (Log2Female-Log2Male)
B
Mouse Sab mRNA 5' A G C C A G G T A C A A C G C T G C C 3'
miR-34a-5p 3' U U G G U C G A U U C U G U G A C G G 5'
C
Relative expression of miR-34a-5p / miR-191-5p
Male
Female
D
HEK293
C
miR34a-5p
SAB
GAPDH
E
Liver
Male
Female
p53
ERα
GAPDH
P53 / GAPDH
F
Liver
Men
Women
p53
β-Actin
P53 / β-actin
G
Liver
Male
Female
Veh
PPT
Fulv
p53
GAPDH
P53 / GAPDH

Figure 5. ERα and p53 regulation of miR34a-5p expression. (A) Liver from male and female littermates were snap frozen in RNA*later* RNA stabilizing solution and miRNA seq analysis was performed. N = 3 mice per group. Volcano plot of fold change difference of miRNA expression in female versus male mice liver was shown. *Sab* targeting *miR34a-5p* was expressed 3.2 fold significantly higher level in female than male littermates. Log_2FC (0.59) or (-0.59) is equivalent to 1.5 fold change expression either direction. **(B)** *miR34a-5p* and *Sab* mRNA alignment. **(C)** qPCR analysis of *miR34a-5p* expression. *miR191-5p* expression in RNAseq analysis was not different in male versus female and used as a loading control. N=5 mice in each group, (∗) = P<0.05 vs male, by un-paired, 2-tailed Student's *t* test. **(D)** *miR-34a-5p* mimic was transfected to HEK293 cells and cultured for 3 days. Cell survival was the same as non-transfected cells (data not shown). SAB level was determined by immunoblot using rabbit anti-SAB. For control "C", cells were transfected with scrambled oligo. (<) indicates non-specific band. **(E, F)** Basal level of expression of p53, ERα protein was determined in male vs female littermates (N=10 mice per group, (∗) = P<0.05 vs male, by un-paired, 2-tailed Student's *t* test) and human livers of males and premenopausal females. N=5 pairs. (∗) = P<0.05 vs men, by paired, 2-tailed Student's *t* test. **(G)** Male mice were treated with PPT to activate ERα, and female mice were treated with fulvestrant to deplete ERα. Liver protein extract was examined for p53 expression. Representative immunoblot of 3 separate experiments. N=3 per group. (∗) = *P* <0.05 versus vehicle control (veh) male; (#) = *P* <0.05 versus vehicle control female, by un-paired, 2-tailed Student's *t* test. All data are presented as the mean ± SEM.

Figure 6

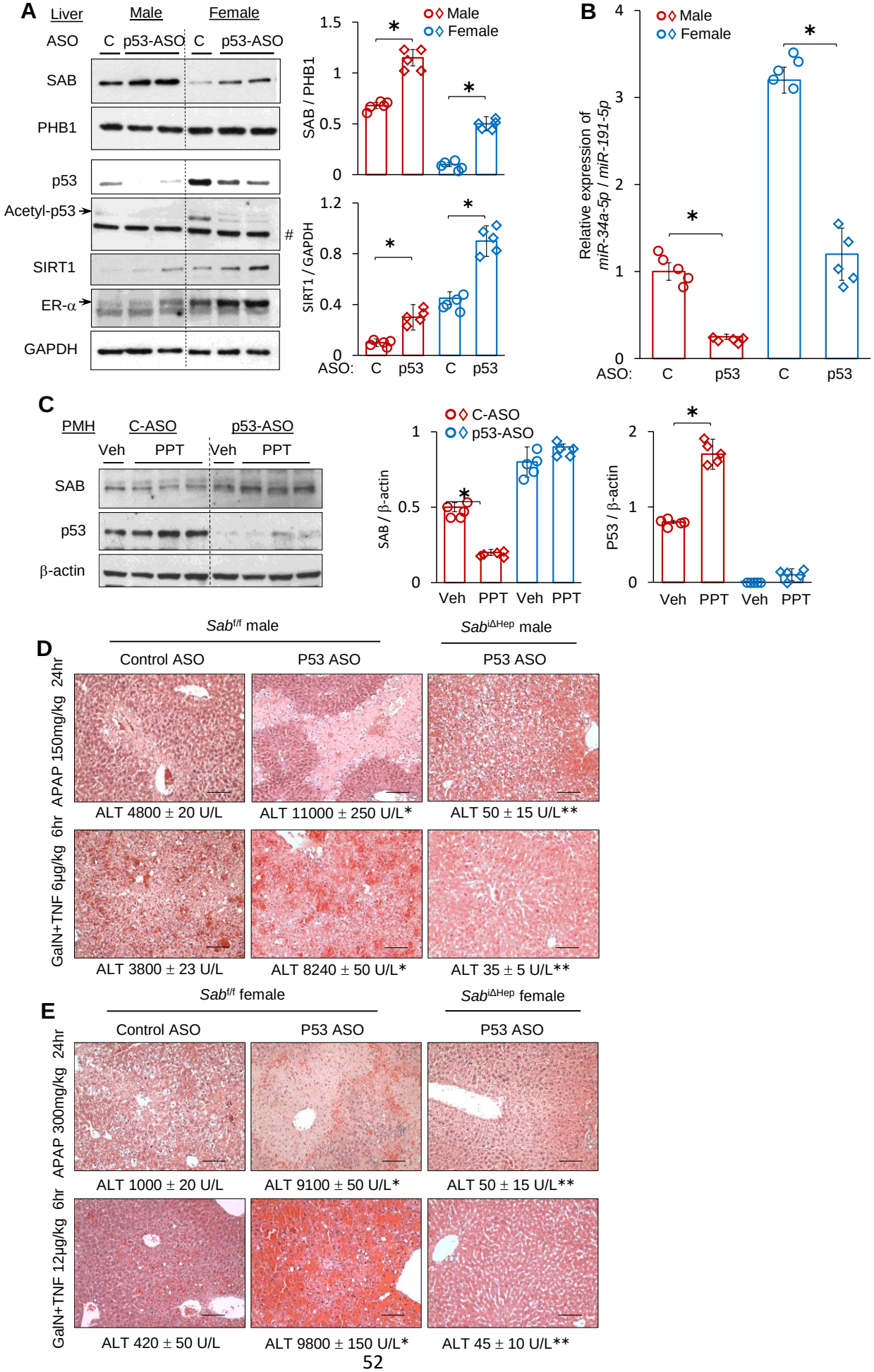
A
Liver
Male
Female
ASO
C
p53-ASO
C
p53-ASO
SAB
PHB1
p53
Acetyl-p53
SIRT1
ER-α
GAPDH
#
Male
Female
SAB / PHB1
SIRT1 / GAPDH
ASO: C p53 C p53
B
Male
Female
Relative expression of miR-34a-5p / miR-191-5p
ASO: C p53 C p53
C
PMH
C-ASO
p53-ASO
Veh
PPT
Veh
PPT
SAB
p53
β-actin
C-ASO
p53-ASO
SAB / β-actin
P53 / β-actin
Veh PPT Veh PPT
D
Sab f/f male
Sab iΔHep male
Control ASO
P53 ASO
P53 ASO
APAP 150mg/kg 24hr
ALT 4800 ± 20 U/L
ALT 11000 ± 250 U/L*
ALT 50 ± 15 U/L**
GalN+TNF 6μg/kg 6hr
ALT 3800 ± 23 U/L
ALT 8240 ± 50 U/L*
ALT 35 ± 5 U/L**
E
Sab f/f female
Sab iΔHep female
Control ASO
P53 ASO
P53 ASO
APAP 300mg/kg 24hr
ALT 1000 ± 20 U/L
ALT 9100 ± 50 U/L*
ALT 50 ± 15 U/L**
GalN+TNF 12μg/kg 6hr
ALT 420 ± 50 U/L
ALT 9800 ± 150 U/L*
ALT 45 ± 10 U/L**

Figure 6. p53 modulates hepatotoxicity through SAB expression. Ten to twelve week old littermate male or female mice received scramble control [C] or *p53* ASO (50mg/kg i.p) 7 doses over two weeks. **(A, B)** SAB and PHB1 expression was determined in mitochondrial fraction. p53, acetyl-p53, SIRT1, ER-α and GAPDH were determined in whole liver extracts. Representative immunoblot of 3 separate experiments. *miR-34a-5p* was quantitated by qPCR. N=5 mice in each group. (∗) = *P* <0.05 versus control ASO [C], by un-paired, 2-tailed Student's *t* test. Data are presented as the mean ± SEM. **(C)** Male PMH from scrambled control or *p53* ASO were treated with DMSO [Veh] or PPT 10μM for 2days. Representative immunoblot of 3 separate experiments. N=5 mice in each group. (∗) = *P* <0.05 versus vehicle control (veh), by un-paired, 2-tailed Student's *t* test. Data are presented as the mean ± SEM. **(D, E)** Scrambled control or *p53* ASO treated *Sab*$^{f/f}$ or *Sab*$^{i\Delta Hep}$ male or female mice were fasted overnight and treated with APAP (150 or 300mg/kg i.p) or galactosamine (GalN, 800mg/kg i.p) and TNF-α (6 or 12μg/kg i.p), and 24 hrs or 6hrs later, respectively, liver histology and serum ALT were determined. Representative H&E stained image. Original magnification: x20. Scale bars: 100μm. N=3 mice in Control ASO group and 5 mice in p53 ASO groups. (∗) = *P* <0.05 versus control ASO group; (∗∗) = *P* <0.05 versus p53ASO+*Sab*$^{f/f}$, by un-paired, 2-tailed Student's *t* test. Data are presented as the mean ± SD.

Figure 7

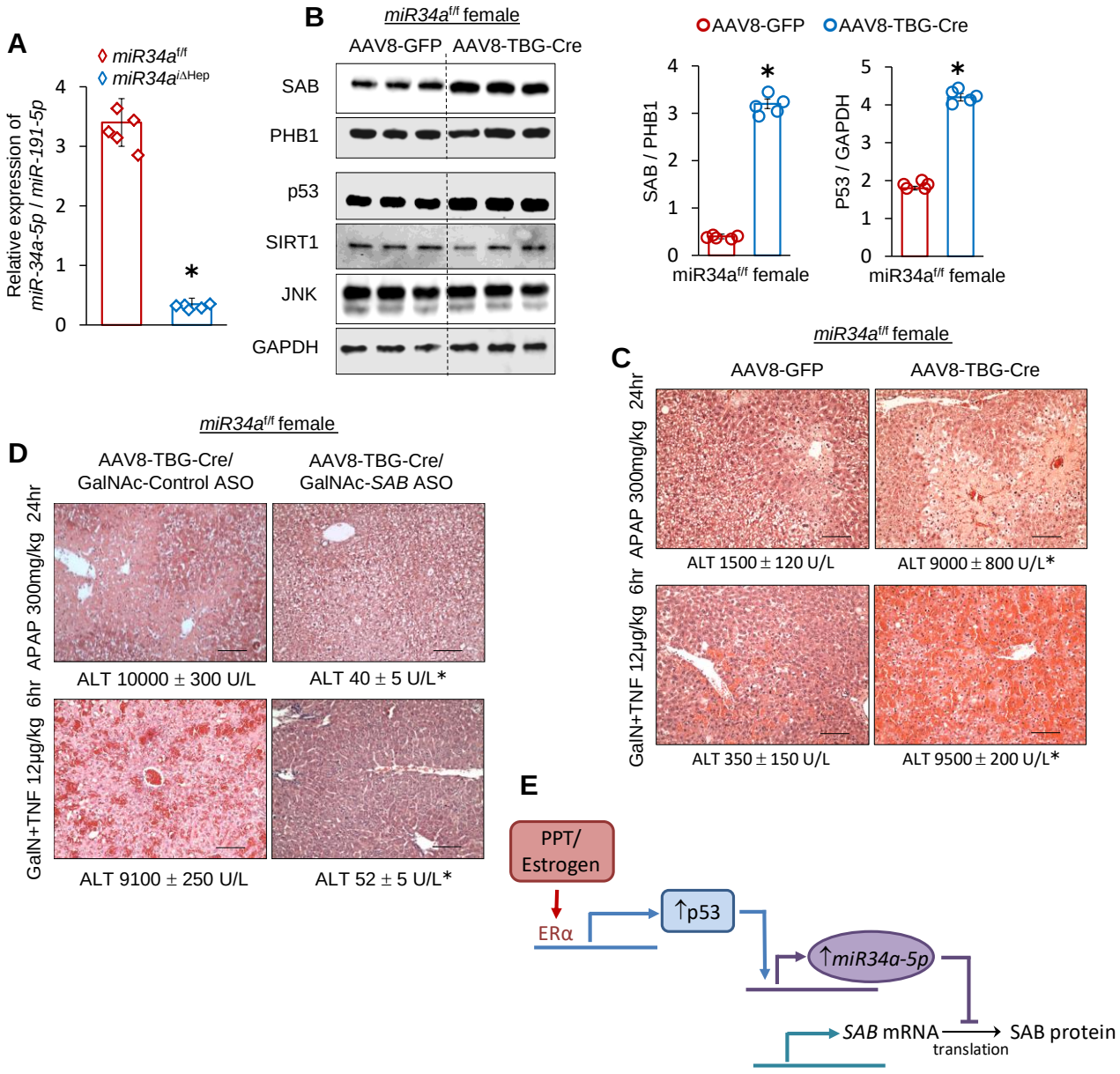
A
miR34a f/f
miR34a iΔHep
Relative expression of miR-34a-5p / miR-191-5p
B
miR34a f/f female
AAV8-GFP AAV8-TBG-Cre
SAB
PHB1
p53
SIRT1
JNK
GAPDH
AAV8-GFP AAV8-TBG-Cre
SAB / PHB1
P53 / GAPDH
miR34a f/f female
C
miR34a f/f female
AAV8-GFP
AAV8-TBG-Cre
24hr APAP 300mg/kg
6hr GalN+TNF 12µg/kg
ALT 1500 ± 120 U/L
ALT 9000 ± 800 U/L*
ALT 350 ± 150 U/L
ALT 9500 ± 200 U/L*
D
miR34a f/f female
AAV8-TBG-Cre/ GalNAc-Control ASO
AAV8-TBG-Cre/ GalNAc-SAB ASO
24hr APAP 300mg/kg
6hr GalN+TNF 12µg/kg
ALT 10000 ± 300 U/L
ALT 40 ± 5 U/L*
ALT 9100 ± 250 U/L
ALT 52 ± 5 U/L*
E
PPT/ Estrogen
ERα
↑p53
↑miR34a-5p
SAB mRNA
translation
SAB protein

Figure 7. miRNA-34a-5p modulates SAB expression and hepatotoxicity. *miR34a*$^{f/f}$ female mice received AAV8-TBG-GFP or AAV8-TBG-Cre through tail vein injection to generate *miR34a*$^{f/f}$ or *miR34a*$^{i\Delta Hep}$. 2 weeks later **(A, B)** *miR34a-5p* expression, SAB and PHB1 expression in mitochondria, p53, SIRT1 and GAPDH in liver extract were determined. N=5 mice in each group. (∗) = *P* <0.05 versus AAV8-GFP group, by un-paired, 2-tailed Student's *t* test. Data are presented as the mean ± SEM. **(C)** Overnight fasted mice received APAP or GalN/TNF and liver histology and serum ALT at 24hr or 6hr respectively were examined**.** Representative H&E stained image. Original magnification: x20. Scale bars: 100μm. N=5 mice in each group. (∗) = *P* <0.05 versus AAV8-GFP group, by un-paired, 2-tailed Student's *t* test. Data are presented as the mean ± SD. **(D)** *miR34a*$^{i\Delta Hep}$ (*miR34a*$^{f/f}$+AAV8-TBG-Cre) female mice received GalNAc-Control or *Sab* ASO for two weeks to deplete hepatocellular SAB expression. Overnight fasted mice then received APAP or GalN/TNF and liver histology and serum ALT at 24hr or 6hr respectively were examined**.** Representative H&E stained image. Original magnification: x20. Scale bars: 100μm. N=5 mice in each group. (∗) indicates p <0.05 versus GalNAc-Control ASO, by un-paired, 2-tailed Student's *t* test. Data are presented as the mean ± SD. **(E)** Schematic presentation of ERα – p53 – *miR34a-5p* axis of regulation of SAB expression.